processes

MDPI

Article

Research on Flow Characteristics of Straight Line Conjugate Internal Meshing Gear Pump

Hongqiang Chai [1,2,*], Guolai Yang [1,2,*], Guoguo Wu [1,3,*], Guixiang Bai [1] and Wenqi Li [4]

1 College of Energy and Power Engineering, Lanzhou University of Technology, Lanzhou 730050, China; bai04guixiang@126.com
2 State Key Laboratory of Fluid Power and Mechatronic Systems, Zhejiang University, Hangzhou 310027, China
3 School of Intelligent Manufacturing Engineering, Chongqing University of Arts and Sciences, Chongqing 402160, China
4 Lanzhou Ls Group Co., Ltd., Lanzhou Ls Energy Equipment Engineering Research Institute Co., Ltd. Gansu Intelligent Control & Key Laboratory of Metal Plasticity Forming Equipment, Lanzhou 730314, China; li04wenqi@126.com
* Correspondence: chaihq35@163.com (H.C.); yanggl@lut.cn (G.Y.); wuguoguo@cqwu.edu.cn (G.W.)

Received: 9 January 2020; Accepted: 21 February 2020; Published: 27 February 2020

Abstract: The improvement of the overall performance of hydraulic pumps is the basis of intelligent hydraulics. Taking the straight line conjugate internal meshing gear pump as the research object, the theoretical flow rate and the geometric flow pulsation rate equations are established in this study through the volume change method. The change laws of the gear pair's geometric parameters on the theoretical flow rate and the geometric flow pulsation rate are studied. The simulation model of the internal flow channel is established, and the influence factors and the influence degree of the flow pulsation and average flow rate are analyzed. The high-pressure positive displacement pump test system is also designed and built. The performance evaluations are conducted, and the experimental results are analyzed. The results show that the periodic change of the meshing point position is the root cause of the geometric flow pulsation. The theoretical flow rate and the geometric flow pulsation rate are 103.71 L/min and 1.76%, respectively. To increase the theoretical flow rate whilst decreasing the geometric flow pulsation rate, the tip circle radius of the external gear should be increased as much as possible within the allowable range of the design calculation. Amongst the three influencing factors that produce flow pulsation, the oil compressibility has no effect on the flow pulsation. The uneven internal leakage is the main factor, and the geometric flow pulsation only accounts for a small proportion. The internal leakage reduces the simulated flow rate by 3.59 L/min. The difference between the experimental and simulated flow rates is less than 2%. Within the allowable speed range, the rotation speed of the external gear should be increased as much as possible to increase the average flow rate and the volumetric efficiency.

Keywords: straight line conjugate internal meshing gear pump; average flow rate; flow pulsation; gear pair's geometric parameters; simulation analysis; performance evaluations

1. Introduction

With the continuous development of hydraulic technology, digital and intelligent hydraulics have become hotspots in the industry. The advancement of the body part and the improvement of the hydraulic pump's overall performance (e.g., high pressure, low noise, low pulsation, and large and variable displacements) are also an objective of intelligent hydraulics [1–5]. The average flow rate, flow pulsation and internal flow field distribution are collectively referred to as the flow characteristics of gear pumps, which are the key factors affecting the large displacement, low pulsation, and low

noise. These flow characteristics should be accurately determined for the research and development of high-performance gear pumps.

The straight line conjugate internal meshing gear pump is a gear pump with a novel design and has an advanced international level. The related patent appeared in 1970 [6]. The core components include an external gear with a straight tooth profile. Its internal ring gear has a high-order circular tooth profile and is conjugate to the straight tooth profile of the external gear. Given unfavourable factors such as the technical protection of foreign companies, open and complete standardised design systems are scarce. Numerous domestic companies and scholars have researched and optimized the design of straight line conjugate internal meshing gear pumps, mainly focusing on derivation of various equations and parameter optimization. Few studies on the performance of the entire pump have been published.

The tooth profile of the gear pair determines the key performance of gear pumps [7]. Ample research has been performed on the derivation of the tooth profile curve and meshing line equations and the optimization of the tooth profile's basic parameters using relevant constraints. Some scholars used the tooth profile normal method to derive the conjugate tooth profile curve and meshing line equations [8–12]. Xu et al. utilized the complex vector method to achieve similar objectives, whereas Wei et al. and Yang et al. employed the general tooth profile normal inversion and meshing angle function methods, respectively [13–15]. Some scholars established the mathematical models for multi-objective optimization and different interferences. By setting the continuous transmission conditions, meshing angles, absence of interference of tooth profile overlap, tooth tip thickness, and tip circle limit radius as the constraint functions, the researchers have investigated the influence of the gear pair's main parameters on the objective function, and optimized the relevant parameters [16–19]. However, the research on multi-objective optimization only focuses on a few sets of data, and does not analyze the optimal value of the objective function in a given interval.

Tooth surface contact transmission is an important source of mechanical vibration noise, which affects tooth surface strength and life [20–22]. Therefore, the analysis of tooth surface meshing and tooth surface contact strength are reported in numerous studies in the literature. Some scholars have established the sliding coefficient equation based on the polar coordinate method, developed the meshing efficiency equation using the tangential polar coordinate method, and used the finite element method to simulate the contact strength of tooth surface and pump's body structure, respectively. The influence of the relevant parameters on the objective function has been analyzed [23–26]. Some scholars established the coincidence degree equations on the basis of the basic law of tooth profile meshing and discussed the corresponding influence of relevant parameters [27,28].

The noise induced by the oil trap phenomenon and the pressure shock noise caused by the flow pulsation are the main noise sources of gear pumps [29–32]. Therefore, research on the mechanism of gear pump vibration and noise reduction is not only a key topic in the field, but also the interest of internationally renowned manufacturers that heavily invest in research. Wang et al. established the instantaneous oil trap volume equation based on the changes in the oil trap volume, and analyzed the influence of relevant parameters [33]. Some scholars established the instantaneous flow rate equations using the gear meshing principle, and derived the approximate equations of flow pulsation rate using the theoretical flow rate approximation equations [34–36]. However, the instantaneous flow rate equation is a general equation and does not change based on the distance from the node to the meshing point and the rotation angle of the external gear. In addition, error exists between the approximate and the exact equations of theoretical flow rate and flow pulsation rate, resulting in an inaccurate reflection of the true value. With respect to the magnitude of the error, no simulation analysis and experimental verification have been performed according to the parameters of the actual model. Similarly, whether the gear pair's geometric parameters change the theoretical flow rate and geometric flow pulsation rate has not been investigated. The development and design of the products should be equipped with the corresponding process equipment for computer-aided design [37]. With regard to the research on the machining method of gear pairs, Zhang et al. proposed a forming method for large-modulus internal

gears. The external gear meshing with the internal gear was matched according to the conjugate principle [38].

None of the above-mentioned studies have performed the numerical simulation of the internal flow channel simulation model to obtain the flow characteristics of the internal flow field, nor analyzed the influence factors and influence degree of the outlet flow pulsation and average flow rate. Moreover, the performance evaluations of straight line conjugate internal meshing gear pumps are not executed using a high-pressure positive displacement pump test system, and the difference between the experimental and simulation results is not investigated.

The flow characteristics of a straight line conjugate internal meshing gear pump should be analyzed to provide reliable data to the designer for an accurate calculation of theoretical flow rate and geometric flow pulsation rate, and provide theoretical foundation to increase the geometric displacement, decrease the flow pulsation to reduce the pressure shock noise and improve the overall performance of gear pumps comprehensively. Based on these, this paper is conducted from three aspects. In terms of theoretical analysis, a general mathematical model of the theoretical instantaneous flow rate is established using the volume change method. By using the number-shape combination method, the theoretical instantaneous flow rate equations based on changes in the distance from the node to the meshing point and the rotation angle of the external gear, the theoretical flow rate equation, and the geometric flow pulsation rate equation are analyzed and determined. Taking the straight line conjugate internal meshing gear pump as the research object, the specific values of the theoretical flow rate and the geometric flow pulsation rate are calculated and analyzed. The design variables affecting theoretical flow rate and geometric flow pulsation rate and the corresponding value ranges are determined, and the change laws of the gear pair's geometric parameters on theoretical flow rate and geometric flow pulsation rate are studied. In terms of numerical simulations, the simulation model of the internal flow channel is developed. The numerical simulation results are analyzed and compared, and the influence factors and the influence degree of the flow pulsation and the average flow rate at the outlet of the gear pump are investigated. In terms of experimental researches, a high-pressure positive displacement pump test system is also designed and built. The performance evaluations for the test pump are implemented, and the experimental results are analyzed and compared with the simulation results.

2. Modeling of the Theoretical Flow Rate and Geometric Flow Pulsation Rate of a Straight Line Conjugate Internal Meshing Gear Pump

2.1. Tooth Profile Curve of the External Gear

The tooth profile curve of the external gear is a left-right symmetric straight line, which is established at the center O_1 of the external gear as the coordinate origin, as shown in Figure 1. The equation of l can be obtained from the geometric relationship of Figure 1.

$$l = r_1 \sin\left(\frac{\theta}{2} + \beta\right) \tag{1}$$

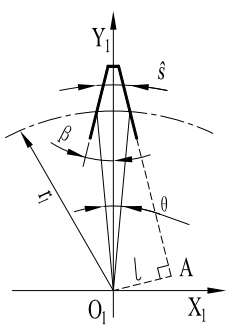

Figure 1. Tooth profile curve of the external gear.

2.2. General Mathematical Model Analysis of Theoretical Instantaneous Flow Rate

The theoretical instantaneous flow rate is established using the volume change method. The working dynamic diagram of straight line conjugate internal meshing gear pump is shown in Figure 2, where k is the meshing point. During the meshing process of the external gear and internal gear ring, the tooth profiles m, n, g, k of the external gear and the tooth profiles k, g', n', m' of the internal gear ring enclose an oil discharge chamber. When the external gear rotates, the full tooth profiles mn and $m'n'$ compress the oil in the oil discharge chamber to make the volume of oil discharge chamber smaller, while the other part of meshing tooth profiles gk and $g'k$ expand the volume of oil discharge chamber during continuous rotation. However, the rest tooth profiles that are completely surrounded by the high-pressure oil do not participate in the work and have no effect on the oil discharge.

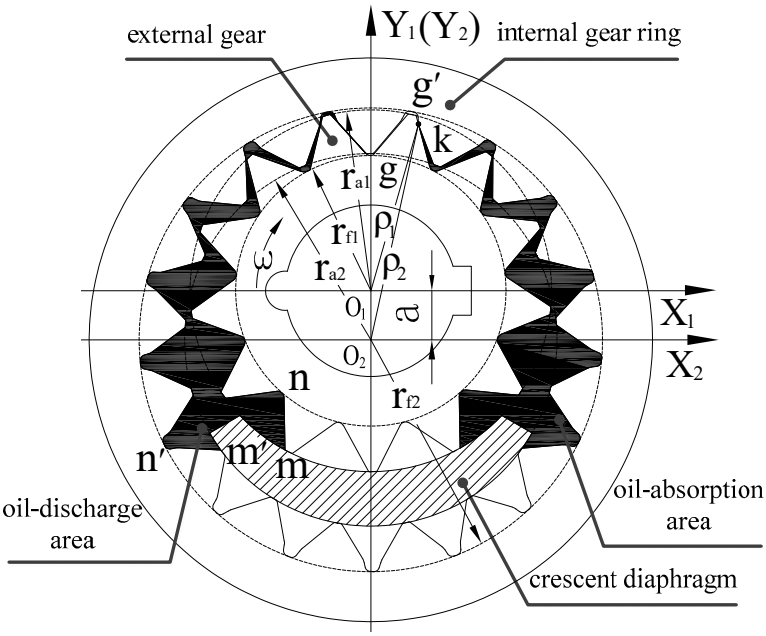

Figure 2. Working dynamic diagram of the straight line conjugate internal meshing gear pump.

Firstly, the sweep area method is used to calculate the volume change of oil discharge chamber. According to the above description, and given that the transmission ratio of the internal meshing gear pair is a fixed value, after the rotation angles of the external gear and the internal gear ring are $\Delta\varphi_1$ and $\Delta\varphi_2$, respectively, it can be obtained from Figure 2 that the full tooth profiles mn and $m'n'$ reduce the volume of oil discharge chamber.

$$\Delta V_1 = \frac{B}{2}\left[\left(r_{a1}^2 - r_{f1}^2\right)\Delta\varphi_1 + \left(r_{f2}^2 - r_{a2}^2\right)\Delta\varphi_2\right] \tag{2}$$

Meanwhile, due to the rotation of the meshing tooth profiles gk and $g'k$, it can be obtained from Figure 2 that the meshing tooth profiles gk and $g'k$ expand the volume of oil discharge chamber.

$$\Delta V_2 = \frac{B}{2}\left[\left(\rho_1^2 - r_{f1}^2\right)\Delta\varphi_1 + \left(r_{f2}^2 - \rho_2^2\right)\Delta\varphi_2\right] \tag{3}$$

According to the meshing principle of tooth profile, the position of the meshing point k constantly changes during working process. In other words, the values of ρ_1 and ρ_2 are not fixed, and they periodically change with the meshing point position. As a result, ΔV_2 also changes periodically, which is the root cause of the geometric flow pulsation. Therefore, in theory, the pulsation of the output instantaneous flow of gear pump is unavoidable.

The volume change of the oil discharge cavity can be obtained by subtracting Equations (2) and (3), which is expressed by Equation (4):

$$\Delta V = \frac{B}{2}\left[\left(r_{a1}^2 - \rho_1^2\right)\Delta\varphi_1 + \left(\rho_2^2 - r_{a2}^2\right)\Delta\varphi_2\right] \tag{4}$$

Equation (5) can be obtained from the basic law of the tooth profile meshing:

$$i_{12} = \frac{\omega_1}{\omega_2} = \frac{\Delta\varphi_1}{\Delta\varphi_2} = \frac{Z_2}{Z_1} = \frac{r_2}{r_1} \tag{5}$$

Equation (5) is substituted into the volume change Equation (4), and the theoretical instantaneous flow rate equation of straight line conjugate internal meshing gear pump can be obtained by derivation and simplification:"

$$q_{sh} = \frac{B\omega_1}{2}\left[r_{a1}^2 - \rho_1^2 + \left(\rho_2^2 - r_{a2}^2\right)\frac{Z_1}{Z_2}\right] \tag{6}$$

From the above analysis, it can be obtained that gear pumps with different tooth profiles exhibit different flow pulsation characteristics due to the different change laws of meshing point position. Further, the change laws can be determined based on the distance from the node to the meshing point and the rotation angle of the external gear.

2.3. Theoretical Instantaneous Flow Rate Equation Based on the Distance Change from the Node to the Meshing Point

According to the meshing principle of the gear pair, the schematic diagram of meshing point's position change is established in the internal meshing gear pair, as shown in Figure 3. By expressing ρ_1 and ρ_2 from the geometric relationship in Figure 3, the theoretical instantaneous flow rate equation based on the distance change from the node to the meshing point can be obtained:

$$q_{sh} = \frac{B\omega_1}{2}\left[r_{a1}^2 - i_{12}^{-1}r_{a2}^2 + (i_{12} - 1)r_1^2 - \left(1 - i_{12}^{-1}\right)f^2\right] \tag{7}$$

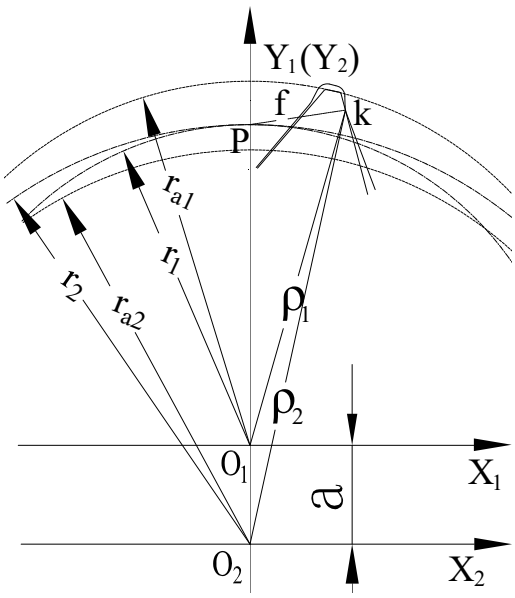

Figure 3. Meshing point's position change.

From the continuous contact transmission's conditions of the tooth profile, it can be known that transmission ratio $i_{12} > 1$ in the internal meshing gear pair, that is, the value of expression $1 - i_{12}^{-1}$ is a

positive number less than 1. Therefore, when f is 0, that is, when the node coincides with the meshing point, the instantaneous flow rate reaches the maximum; when f is maximum, it is at the minimum. At this time, the meshing point may be located at the position where the gear pair is about to enter or exit the meshing. The specific location is discussed in detail in the following section.

2.4. Theoretical Instantaneous Flow Rate Equation Based on the Rotation Angle Change of the External Gear

The schematic diagram of the rotation angle change of the external gear is established according to the definitions of tooth profile parameters, as shown in Figure 4. According to the basic theorem of the tooth profile meshing (i.e., the common normal of two conjugate tooth profiles at the contact point passes through the instantaneous velocity center), in other words, the line between the meshing point and the node is perpendicular to the external gear's profile curve. Based on this and according to the geometric relationship in Figure 4, the equation sets about ρ_1 and ρ_2 can be obtained:

$$\left.\begin{aligned} \rho_1^2 &= l^2 + r_1^2\cos^2(\beta-\varphi) \\ \rho_2^2 &= [a\sin(\beta-\varphi)+l]^2 + r_2^2\cos^2(\beta-\varphi) \end{aligned}\right\} \tag{8}$$

By substituting the Equation (8) into Equation (6), the theoretical instantaneous flow rate equation based on the rotation angle change of the external gear can be obtained:

$$\begin{aligned} q_{sh} \;=\; & \tfrac{B\omega_1}{2}\Big[\left(r_1^2 + i_{12}^{-1}a^2 - i_{12}r_1^2\right)\sin^2(\beta-\varphi) + 2i_{12}^{-1}al\sin(\beta-\varphi) + r_{a1}^2 + i_{12}r_1^2 + i_{12}^{-1}l^2 - \ldots \\ & i_{12}^{-1}r_{a2}^2 - r_1^2 - l^2\Big] \end{aligned} \tag{9}$$

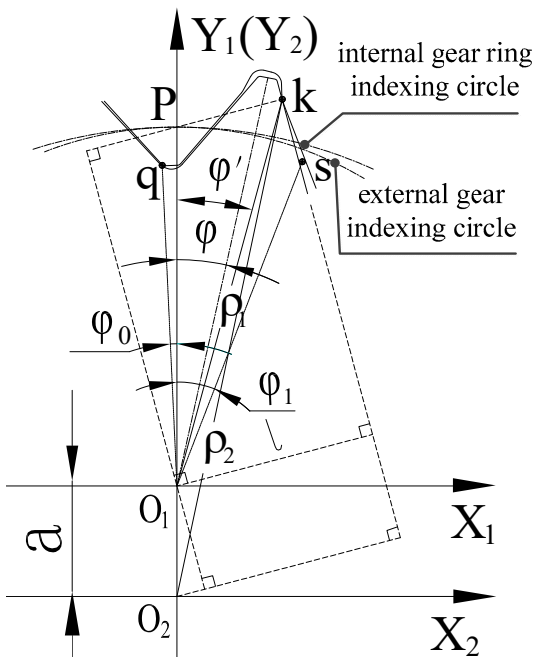

Figure 4. Rotation angle change of the external gear.

2.5. Theoretical Flow Rate Equation of the Straight Line Conjugate Internal Meshing Gear Pump

2.5.1. Theoretical Coincidence Degree Equation and Theoretical Oil Trap Time Equation Based on the Rotation Angle Change of the External Gear

From the meshing process of gear pair [39], it can be known that the starting point when the gear pair enters the meshing is the intersection of the tip circle of internal gear ring and the meshing line, corresponding to the initial meshing angle is φ_0. When the meshing reaches the intersection of

the tip circle of the external gear and the meshing line, the gear pair are about to exit the meshing, which corresponds to the ending meshing angle is φ_1. Based on this and combined with Equation (8), the Equation (10) can be obtained:

$$\left.\begin{aligned} r_{a1}^2 &= l^2 + r_1^2\cos^2(\beta-\varphi_1) \\ r_{a2}^2 &= [a\sin(\beta-\varphi_0)+l]^2 + r_2^2\cos^2(\beta-\varphi_0) \end{aligned}\right\} \tag{10}$$

Equation (11) about the meshing angles φ_0 and φ_1 can be obtained from Equation (10):

$$\left.\begin{aligned} \varphi_0 &= \beta - \arcsin\frac{al+\sqrt{a^2l^2-\left(i_{12}^2r_1^2-a^2\right)\left(r_{a2}^2-l^2-i_{12}^2r_1^2\right)}}{i_{12}^2r_1^2-a^2} \\ \varphi_1 &= \beta - \arccos\frac{\sqrt{r_{a1}^2-l^2}}{r_1} \end{aligned}\right\} \tag{11}$$

According to the definition of the theoretical coincidence degree in the meshing process of gear pair, the theoretical coincidence degree Equation (12) can be obtained:

$$\varepsilon_\alpha = \frac{\arcsin\frac{al+\sqrt{a^2l^2-\left(i_{12}^2r_1^2-a^2\right)\left(r_{a2}^2-l^2-i_{12}^2r_1^2\right)}}{i_{12}^2r_1^2-a^2} - \arccos\frac{\sqrt{r_{a1}^2-l^2}}{r_1}}{2\pi/z_1} \tag{12}$$

Furthermore, the theoretical oil trap time Equation (13) can be obtained:

$$T_\alpha = \frac{\arcsin\frac{al+\sqrt{a^2l^2-\left(i_{12}^2r_1^2-a^2\right)\left(r_{a2}^2-l^2-i_{12}^2r_1^2\right)}}{i_{12}^2r_1^2-a^2} - \arccos\frac{\sqrt{r_{a1}^2-l^2}}{r_1}}{\pi n_1/30} \tag{13}$$

2.5.2. Derivation of the Theoretical Flow Rate Equation

It can be known from the Figure 4 that each pair of gear teeth in the gear pair enters the meshing from the starting point q and exits the meshing from the ending point S. That is, in the rotation process of the external gear from the initial to the end meshing angles, one oil discharge cycle is formed. Assuming that the oil discharge volume is $\Delta\Sigma$ during this oil discharge cycle, and according to the definition of instantaneous flow rate, the mathematical model of the oil discharge volume through a single tooth can be obtained:

$$\Delta\Sigma = \int q_{sh}dt \tag{14}$$

By substituting the instantaneous flow rate Equation (9) and integrating Equation (14), the equation of the oil discharge volume by each pair of gear teeth in one oil discharge cycle can be obtained:

$$\begin{aligned} \Delta\Sigma \;=\; & \tfrac{B}{2}\Big\{\left(r_1^2+i_{12}^{-1}a^2-i_{12}r_1^2\right)\Big[\tfrac{1}{2}(\varphi_1-\varphi_0)-\tfrac{1}{4}\sin 2(\varphi_1-\beta)+\tfrac{1}{4}\sin 2(\varphi_0-\beta)\Big]+2i_{12}^{-1}al[\cos(\varphi_1-\beta)-\cos(\varphi_0-\beta)]+\ldots \\ & \left(r_{a1}^2+i_{12}r_1^2+i_{12}^{-1}l^2-i_{12}^{-1}r_{a2}^2-r_1^2-l^2\right)(\varphi_1-\varphi_0)\Big\} \end{aligned} \tag{15}$$

According to the definition of gear pump's displacement (i.e., the displacement is the oil discharge volume when the gear pairs rotate for one cycle), it is assumed that there are a total of teeth participating in meshing drainage within one cycle, thus the theoretical displacement equation can be obtained:

$$\Sigma = \Delta\Sigma z_1 \tag{16}$$

The equation of the theoretical flow rate of straight line conjugate internal meshing gear pump is obtained by combining the initial and ending meshing angles from Equation (11):

$$\begin{aligned} q_t = \ & \tfrac{z_1 n_1 B}{8}\Bigg\{\left(r_1^2 + i_{12}^{-1}a^2 - i_{12}r_1^2\right)\Bigg[2\left(\arcsin\frac{al+\sqrt{a^2l^2-\left(i_{12}^2r_1^2-a^2\right)\left(r_{a2}^2-l^2-i_{12}^2r_1^2\right)}}{i_{12}^2r_1^2-a^2} - \arccos\frac{\sqrt{r_{a1}^2-l^2}}{r_1}\right) + \sin 2\left(\arccos\frac{\sqrt{r_{a1}^2-l^2}}{r_1}\right) - \ldots \\ & 2\left(\frac{al+\sqrt{a^2l^2-\left(i_{12}^2r_1^2-a^2\right)\left(r_{a2}^2-l^2-i_{12}^2r_1^2\right)}}{i_{12}^2r_1^2-a^2}\right)\cos\left(\arcsin\frac{al+\sqrt{a^2l^2-\left(i_{12}^2r_1^2-a^2\right)\left(r_{a2}^2-l^2-i_{12}^2r_1^2\right)}}{i_{12}^2r_1^2-a^2}\right)\Bigg] + \ldots \\ & 8i_{12}^{-1}al\left[\frac{\sqrt{r_{a1}^2-l^2}}{r_1} - \cos\left(\arcsin\frac{al+\sqrt{a^2l^2-\left(i_{12}^2r_1^2-a^2\right)\left(r_{a2}^2-l^2-i_{12}^2r_1^2\right)}}{i_{12}^2r_1^2-a^2}\right)\right] + \ldots \\ & 4\left(r_{a1}^2 + i_{12}r_1^2 + i_{12}^{-1}l^2 - i_{12}^{-1}r_{a2}^2 - r_1^2 - l^2\right)\left(\arcsin\frac{al+\sqrt{a^2l^2-\left(i_{12}^2r_1^2-a^2\right)\left(r_{a2}^2-l^2-i_{12}^2r_1^2\right)}}{i_{12}^2r_1^2-a^2} - \arccos\frac{\sqrt{r_{a1}^2-l^2}}{r_1}\right)\Bigg\} \end{aligned} \tag{17}$$

2.6. Geometric Flow Pulsation Rate Equation of the Straight Line Conjugate Internal Meshing Gear Pump

2.6.1. Maximum and Minimum Analysis of the Theoretical Instantaneous Flow Rate

The equation about φ' can be obtained from the geometric relation in Figure 4:

$$\varphi' = \arcsin\frac{l}{\rho_1} - (\beta - \varphi) \tag{18}$$

From the aforementioned analysis, we can know that when the meshing point coincides with the node, that is, when φ' is equal to 0, the theoretical instantaneous flow rate reaches the maximum, thus the equation of the maximum instantaneous flow rate can be obtained:

$$q_{sh\max} = \frac{B\omega_1}{2}\left[r_{a1}^2 - r_1^2 + \left(i_{12}^2r_1^2 - r_{a2}^2\right)i_{12}^{-1}\right] \tag{19}$$

To obtain the minimum of the theoretical instantaneous flow rate, Equation (9) is derived with respect to the rotation angle φ, and make the derivative function be equal to 0 to solve the equation sets about φ:

$$\left.\begin{aligned} \varphi &= \beta + \left(\tfrac{\pi}{2} + k\pi\right) \\ \varphi &= \beta - \arcsin\tfrac{i_{12}^{-1}al}{i_{12}r_1^2 - r_1^2 - i_{12}^{-1}a^2} + k\pi \end{aligned}\right\} \tag{20}$$

Remove the inappropriate solution and determine the rotation angle of the external gear when the instantaneous flow rate reaches the limit:

$$\varphi_{\lim} = \beta - \arcsin\frac{i_{12}^{-1}al}{i_{12}r_1^2 - r_1^2 - i_{12}^{-1}a^2} \tag{21}$$

By comparison, it is found that Equation (21) is completely consistent with Equation (11) after deformation. Therefore, when the rotation angle of the external gear is the same as the ending meshing angle, the theoretical instantaneous flow rate is at the minimum, further, the minimum instantaneous flow rate equation can be obtained:

$$\begin{aligned} q_{sh\min} \ & = \tfrac{B\omega_1}{2}\Big[\left(r_1^2 + i_{12}^{-1}a^2 - i_{12}r_1^2\right)\sin^2(\beta - \varphi_1) + 2i_{12}^{-1}al\sin(\beta - \varphi_1) + r_{a1}^2 + i_{12}r_1^2 + i_{12}^{-1}l^2 - \ldots \\ & i_{12}^{-1}r_{a2}^2 - r_1^2 - l^2\Big] \end{aligned} \tag{22}$$

2.6.2. Determination of the Geometric Flow Pulsation Rate Equation

According to the definition of the geometric flow pulsation rate (i.e., it is the ratio of the difference between the maximum and minimum instantaneous flow rates to the theoretical flow), which is expressed by an equation:

$$\delta_q = \frac{q_{sh\max} - q_{sh\min}}{q_t} \tag{23}$$

The equations of the maximum and minimum instantaneous flow rates, and the theoretical flow rate are substituted into Equation (23), respectively. Thereby, the equation of the geometric flow pulsation rate of straight line conjugate internal meshing gear pump can be obtained:

$$\begin{aligned}
\delta_q = {} & \frac{8\pi}{z_1}\left[\left(1-i_{12}^{-1}\right)l^2 - 2\left(r_1^2 + i_{12}^{-1}a^2 - i_{12}r_1^2\right)\frac{\sqrt{r_{a1}^2-l^2}}{r_1}\sin\left(\arccos\frac{\sqrt{r_{a1}^2-l^2}}{r_1}\right) - 2i_{12}^{-1}al\sin\left(\arccos\frac{\sqrt{r_{a1}^2-l^2}}{r_1}\right)\right]/\ldots \\
& \left\{\left(r_1^2 + i_{12}^{-1}a^2 - i_{12}r_1^2\right)\left[2\left(\arcsin\frac{al+\sqrt{a^2l^2-\left(i_{12}^2r_1^2-a^2\right)\left(r_{a2}^2-l^2-i_{12}^2r_1^2\right)}}{i_{12}^2r_1^2-a^2} - \arccos\frac{\sqrt{r_{a1}^2-l^2}}{r_1}\right) + \sin 2\left(\arccos\frac{\sqrt{r_{a1}^2-l^2}}{r_1}\right) - \ldots\right.\right. \\
& \left.2\left(\frac{al+\sqrt{a^2l^2-\left(i_{12}^2r_1^2-a^2\right)\left(r_{a2}^2-l^2-i_{12}^2r_1^2\right)}}{i_{12}^2r_1^2-a^2}\right)\cos\left(\arcsin\frac{al+\sqrt{a^2l^2-\left(i_{12}^2r_1^2-a^2\right)\left(r_{a2}^2-l^2-i_{12}^2r_1^2\right)}}{i_{12}^2r_1^2-a^2}\right)\right] + \ldots \\
& 8i_{12}^{-1}al\left[\frac{\sqrt{r_{a1}^2-l^2}}{r_1} - \cos\left(\arcsin\frac{al+\sqrt{a^2l^2-\left(i_{12}^2r_1^2-a^2\right)\left(r_{a2}^2-l^2-i_{12}^2r_1^2\right)}}{i_{12}^2r_1^2-a^2}\right)\right] + \ldots \\
& \left.4\left(r_{a1}^2 + i_{12}r_1^2 + i_{12}^{-1}l^2 - i_{12}^{-1}r_{a2}^2 - r_1^2 - l^2\right)\left(\arcsin\frac{al+\sqrt{a^2l^2-\left(i_{12}^2r_1^2-a^2\right)\left(r_{a2}^2-l^2-i_{12}^2r_1^2\right)}}{i_{12}^2r_1^2-a^2} - \arccos\frac{\sqrt{r_{a1}^2-l^2}}{r_1}\right)\right\}
\end{aligned} \tag{24}$$

3. Simulation Analysis of the Flow Characteristics of a Straight Line Conjugate Internal Meshing Gear Pump

Taking the straight line conjugate internal meshing gear pump as the research object, the specific values of the theoretical flow rate and the geometric flow pulsation rate are calculated and analysed according to gear pair's geometric parameters, and the change laws of gear pair's geometric parameters on the theoretical flow rate and geometric flow pulsation rate are studied. Then, in the case of considering the clearance leakage of the axial and radial, the dynamic grid technology is used to develop the simulation model of the internal flow channel, the distribution of internal flow field is analyzed, and the influence factors and the influence degree of the flow pulsation and the average flow rate at the outlet of the gear pump are investigated.

3.1. Analysis of the Theoretical Flow Rate Curves of a Straight Line Conjugate Internal Meshing Gear Pump

Given the gear pair's basic parameters of the straight line conjugate internal meshing gear pump, the gear pair's geometric parameters can be calculated. The calculation results are shown in Table 1.

Table 1. Geometric parameters of the gear pair.

Name	External Gear	Internal Gear Ring
Number of teeth	13	17
Profile half angle of the external gear (°)	28	
Reference circle diameter (mm)	65	85
Tip circle diameter (mm)	74.5	75.5
Root circle diameter (mm)	54.5	95.5
Center distance (mm)	10	
Actual coincidence degree	1.0288	

The gear pair's geometric parameters in Table 1 are substituted into the theoretical instantaneous flow rate Equation (9) and the initial and ending meshing angles equation sets (11). When the rotation speed is 2000 r/min, the theoretical flow rate curves corresponding to the theoretical coincidence degree can be obtained by programming [40] based on the M language and running the program, as shown in Figure 5.

It can be known from Figure 5 that the theoretical instantaneous flow rate curve changes continuously and periodically, and the curve intersects and distributes in a zigzag shape. The change period is the difference between the ending and initial meshing angles (i.e., the cycle is 0.5419 rad). The instantaneous flow rates corresponding to the ending meshing angle is much smaller than that corresponding to the initial meshing angle. The theoretical average flow rate is distributed horizontally in a straight line. According to Equation (12), the theoretical coincidence degree of the gear pump

is 1.1212. However, the actual coincidence degree is 1.0288. Therefore, when the gear pair exits the meshing, the meshing point is not at the intersection of the tip circle of the external gear and the meshing line, but in advance. Based on this, the theoretical flow rate curves corresponding to actual coincidence degree can be obtained, as shown in Figure 6.

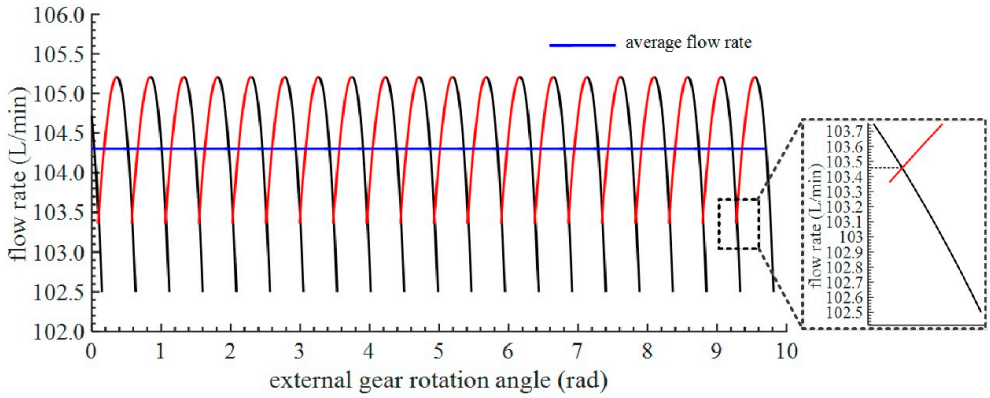

Figure 5. Theoretical flow rate curves corresponding to theoretical coincidence degree.

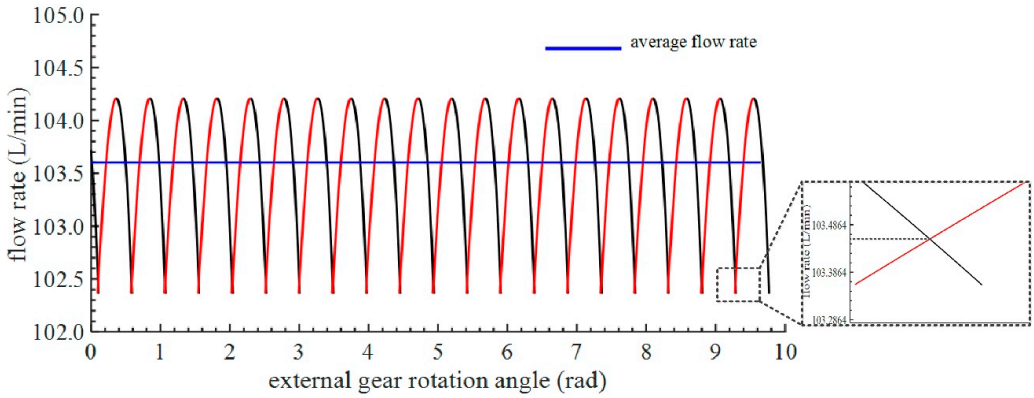

Figure 6. Theoretical flow rate curves corresponding to the actual coincidence degree.

Comparing Figure 5 with Figure 6, it can be known that the theoretical instantaneous flow rate curves correspond to the actual and theoretical coincidence degrees, respectively, are basically the same. The only difference is that the actual ending meshing angle is less than the theoretical, and the corresponding instantaneous flow rates are larger. The instantaneous flow rates corresponding to the initial and ending meshing angles are basically the same. According to Figure 6, the theoretical flow rate and the geometric flow pulsation rate are 103.61 L/min and 1.78%, respectively, whereas the theoretical flow rate and the geometric flow pulsation rate calculated by Equations (17) and (24) are 103.71 L/min and 1.76%, respectively. The difference rates are only 0.1% and 1%, respectively. Such a small error can be ignored. Since the oil compressibility and the internal leakage of the gear pump are not taken into account, the curve of the theoretical instantaneous flow rate is smooth and the geometric flow pulsation rate is low.

3.2. Study on Change Laws of Gear Pair'S Geometric Parameters to the Theoretical Flow Rate and Geometric Flow Pulsation Rate

3.2.1. Design Variables and the Corresponding Value Range

According to the theoretical flow rate Equation (17) and the geometric flow pulsation rate Equation (24), the gear pair's geometric parameters affecting the theoretical flow rate and the geometric flow pulsation rate are gear width, number of the external gear, reference circle radius of the external gear,

center distance, transmission ratio, profile half angle of the external gear, center angle corresponding to tooth thickness of the external gear reference circle, tip circle radius of the external gear, and tip circle radius of internal gear ring, respectively. Given that the gear number combinations in gear pairs with the small gear difference (usually three or four) are several common groups, thus, the gear number should not be used as a design variable. When the reference circle radius of the external gear is determined, the center angle and the center distance are also determined. The effect of the gear width on the flow characteristics is obvious. Therefore, the identified design variables are as follows: reference circle radius of the external gear, tip circle radius of the external gear, tip circle radius of internal gear ring, and the profile half angle of the external gear.

Before simulation calculation, the value ranges of the design variables are determined according to constraint conditions. The corresponding constraint conditions include the limitation of the tooth thickness in the gear tip circle, the continuous transmission condition of gear pair, the limitation of meshing limit point, the limitation of tooth profile overlap interference, etc. The specific results are as follows: the reference circle radius of the external gear is 32.5–38 mm, the tip circle radius of the external gear is 33.25–37.25 mm, the tip circle radius of the internal gear ring is 33.75–40.75 mm, and the profile half angle of the external gear is 28–38°.

3.2.2. Influence of the Geometric Parameters on the Theoretical Flow Rate

The theoretical flow rate is programmed according to Equation (17) in MATLAB, and the change laws of the theoretical flow rate with the corresponding geometric parameters are obtained by running the program. The calculated results are shown in Figure 7.

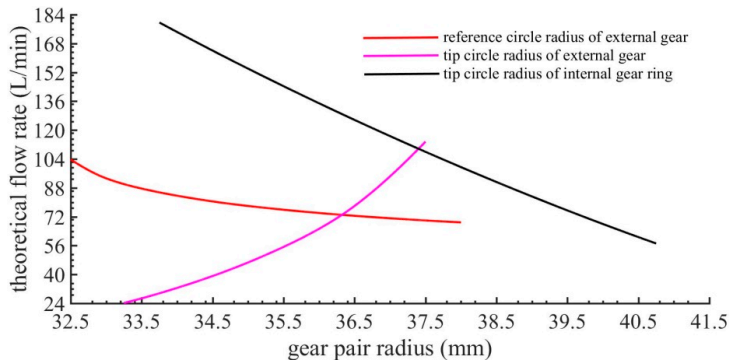

(**a**) With gear pair radius.

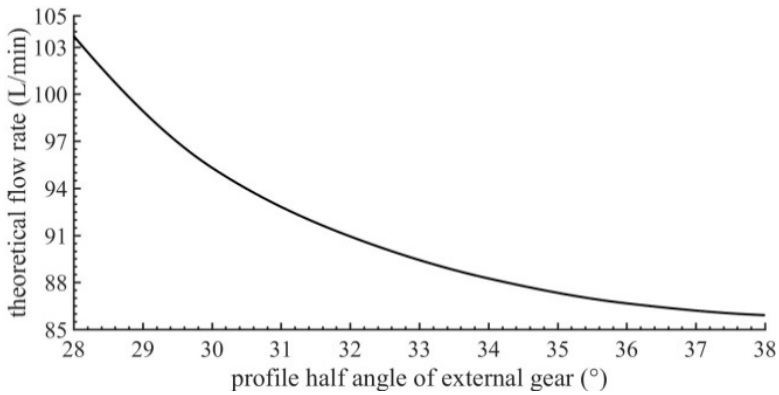

(**b**) With profile half angle of the external gear.

Figure 7. Change laws of the theoretical flow rate.

It can be known from Figure 7 that the theoretical flow rate curves linearly decrease with the increase of the reference circle radius of the external gear, the tip circle radius of internal gear ring and the profile half angle of the external gear, and linearly increases with the increase of the tip circle radius of the external gear. When the tip circle radius of internal gear ring increases 7 mm, the theoretical flow rate decreases by 122 L/min, and the change of the curve is relatively steep. When the reference circle radius of the external gear increases 5.5 mm, the theoretical flow rate decreases by 35 L/min, and the change of the curve is gentle. When the profile half angle of the external gear increases 10°, the theoretical flow rate decreases by 18 L/min, and the change of the curve is very gentle. When the tip circle radius of the external gear increases 4 mm, the theoretical flow rate increases by 79 L/min, and the change of the curve is steep. Therefore, the design variable that exerts the greatest influence on the theoretical flow rate is the tip circle radius of the external gear, and the tip circle radius of internal gear ring is the second.

3.2.3. Influence of the Geometric Parameters on the Flow Pulsation Rate

The geometric flow pulsation rate is programmed according to Equation (24) in MATLAB, and the change laws of the geometric flow pulsation rate with the corresponding geometric parameters are obtained by running the program. The calculated results are shown in Figure 8.

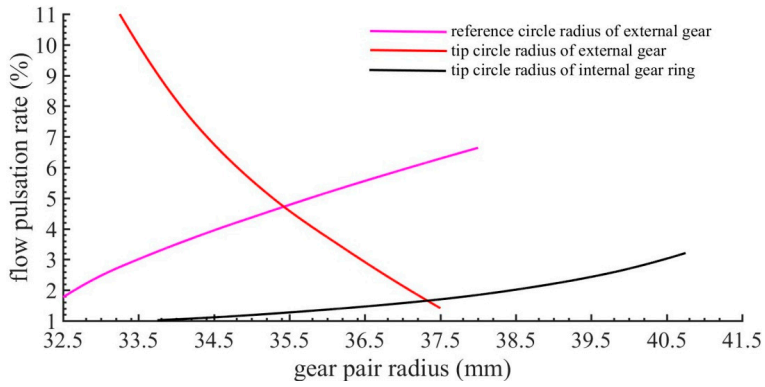

(**a**) With gear pair radius.

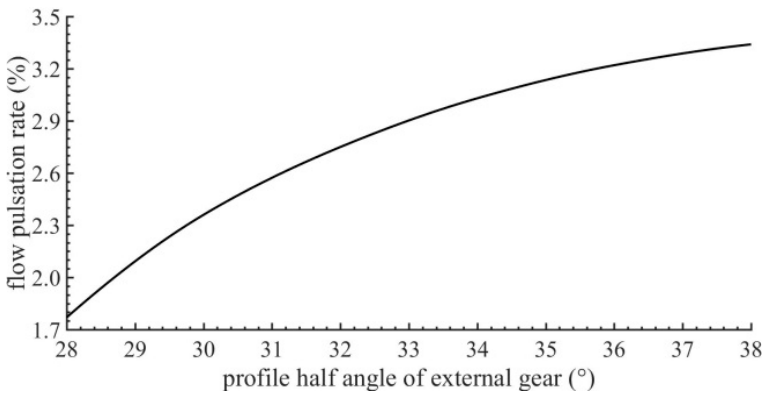

(**b**) With profile half angle of the external gear.

Figure 8. Change laws of the geometric flow pulsation rate.

It can be known from Figure 8 that the geometric flow pulsation rate increases linearly with the increase of the reference circle radius of the external gear, the tip circle radius of internal gear ring and the profile half angle of the external gear, and decreases linearly with the increase of the tip circle radius of the external gear. When the tip circle radius of internal gear ring increases 7 mm, the geometric flow pulsation rate increases by 2.2%, and the change of the curve is very gentle. When the reference circle radius of the external gear increases 5.5 mm, the geometric flow pulsation rate increases by 4.9%,

and the change of the curve is gentle. When the profile half angle of the external gear increases 10°, the geometric flow pulsation rate increases by 1.5%, and the change of the curve is very gentle. When the tip circle radius of the external gear increases 4 mm, the geometric flow pulsation rate decreases by 9.2%, and the change of the curve is steep. Therefore, the design variable that exerts the greatest influence on the geometric flow pulsation rate is the tip circle radius of the external gear.

After analysis and comparisons, it can be concluded that the design variable that exerts the greatest influence on the theoretical flow rate and the geometric flow pulsation rate is the tip circle radius of the external gear. As this radius increases, the theoretical flow rate sharply increases, and the geometric flow pulsation rate sharply decreases. The tip circle radius of internal gear ring only influences the theoretical flow rate, which constantly decreases with the increase in this radius. The remaining variables exert no significant effect on the theoretical flow rate and the geometric flow pulsation rate.

Therefore, to increase the theoretical flow rate whilst decreasing the geometric flow pulsation rate, the tip circle radius of the external gear should be increased as much as possible within the allowable range of the design calculation.

3.3. Establishment of the Simulation Model of Internal Flow Channel

According to the model of the straight line conjugate internal meshing gear pump, the corresponding main characteristic parameters on the sample [41] are listed, as shown in Table 2.

Table 2. Main characteristic parameters.

Displacement (ml/r)	Mximum Speed (r/min)	Outlet Pressure (bar)		Mineral Oil (mm^2/s)
		rating	peak	viscosity range
50.3	2600	125	160	10–100

The schematic diagram of main components in the straight line conjugate internal meshing gear pumpis establish, as shown in Figure 9.

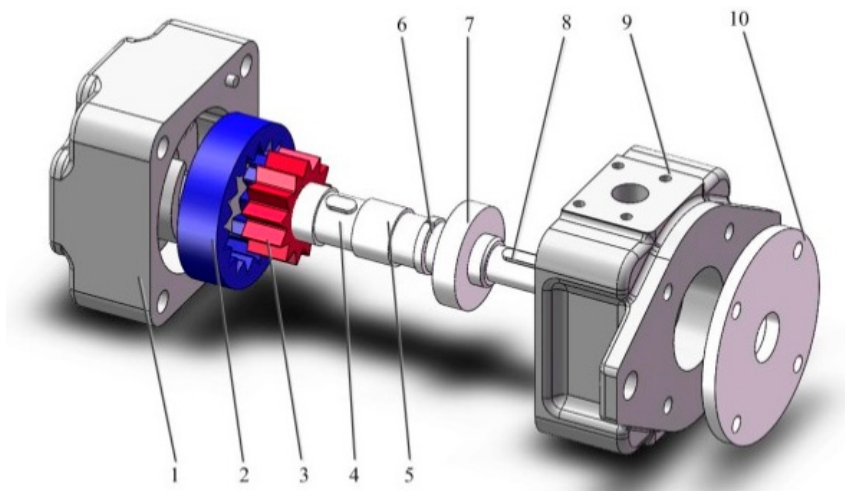

Figure 9. Three-dimensional structure diagram of straight line conjugate internal meshing gear pump: 1–pump body; 2–internal gear ring; 3–external gear; 4–pump shaft; 5–sliding bearing; 6–bearing retaining ring; 7–rolling bearing; 8–ordinary flat key; 9–pump cover; 10–bearing cover.

The sealed cavity in the straight line conjugate internal meshing gear pump is composed of the pump body end face, the internal wall surface, the pump cover end face, the crescent diaphragm side, the external gear bearing surface, and a pair of meshing gear pairs. The internal meshing gear pair is the moving part of gear pumps. The oil transportation function is realized through the meshing transmission of the gear pair.

The internal flow channel model is created and is divided into five parts: oil absorption area, oil discharge area, rotor area, oil distribution area on the absorption side, and oil distribution area on the discharge side, as shown in Figure 10.

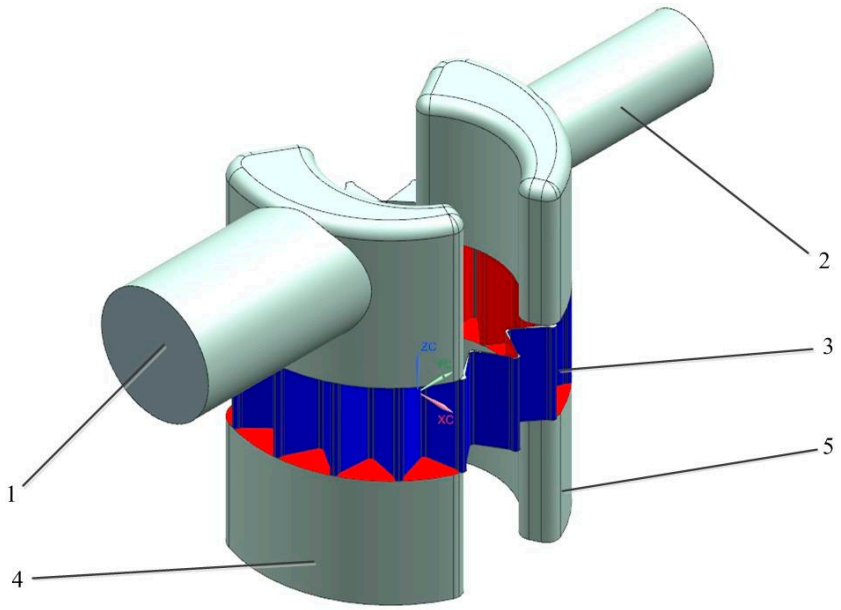

Figure 10. Flow channel model of the straight line conjugate internal meshing gear pump: 1–oil absorption area; 2–oil discharge area; 3–rotor area; 4–oil distribution area on the absorption side; 5–oil distribution area on the discharge side.

In the working process of the gear pump, the friction pairs' surfaces are separated by a certain thickness of oil film to prevent the friction pairs from directly contacting. There are four pairs of friction pairs in the gear pump, respectively, the gear end face and the side plate, the tooth tip, and the shell inner wall surface, between the meshing tooth surfaces, and the bearing and the hub. According to the friction pair design theory of the hydraulic pump and motor [42], the oil film thickness is set as follows: the clearances between the tip circle of the external gear and the crescent diaphragm, and between the tip circle of internal gear ring and the crescent diaphragm are all 20 μm; the gear side clearance is 4 μm; the axial clearance, the radial clearances between the internal ring gear and the shell inner wall surface, and between the bearing and the hub are all 30 μm. The specific oil film thickness is set in the grid model, which is not mentioned here.

The internal flow channel grid model of the gear pump is established [43], that is, the static region uses the geometry conformal adaptive binary-tree algorithm to generate Cartesian grids, which can well adapt to curves and surfaces. The built-in grid generation template is used to generate structured dynamic grid in the dynamic region. The boundaries of different fluid regions (e.g., dynamic regions and static regions) are set as a pair of interfaces by using the mismatched grid interface technology. In this way, each fluid variable passes through the moving surface automatically and implicitly. The mesh quality is aimed at non-broken surface, and the mesh in the rotor area is refined. The grid model is shown in Figure 11.

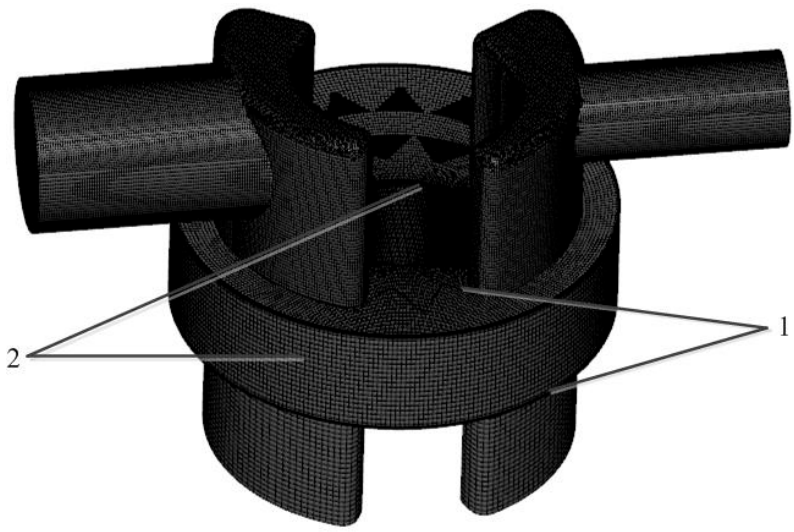

Figure 11. Flow channel grid model of the straight line conjugate internal meshing gear pump: 1–axial clearance; 2–radial clearance.

According to the structural conditions of the straight line conjugate internal meshing gear pump, the crescent internal gear pump model is selected. The rotation speed of the external gear is set to 2000 r/min and the remaining parameters are defined. The turbulence model is selected according to flow conditions. According to the main physical and chemical properties of the oil, the equilibrium dissolved gas model is selected in the cavitation model and the remaining parameters in the model are set.

For definition of boundary condition, since the maximum output flow rate is to be obtained, the inlet and outlet conditions are set to the pressure inlet and pressure outlet, respectively. The pressure values are all defined as 101,325 Pa. Given that the heaters and the heat exchangers are installed in the hydraulic system during normal operation, the temperature range of hydraulic oil is generally controlled at 20–50 °C. Due to short working time during the following experimental research, the temperature difference caused by the system heating can be ignored. In addition, the following experiment was performed under no-load conditions, so the system pressure has no effect on the physical and chemical properties of the oil. Therefore, for 46# mineral oil used in the simulation model, its medium properties are unchanged in the process of calculation, and the specific physical and chemical properties are shown in Table 3.

Table 3. 46# Mineral oil medium properties.

Viscosity Grade	Density	Dynamic Viscosity	Air Solubility	Bulk Elastic Modulus
	(kg/m^3)	(Pa/s)		(GPa)
46	843.7	0.039	1×10^{-5}	1.6

After the pre-processing is defined, the grid is first verified for irrelevance, and verification results are shown in Table 4.

Table 4. Comparison of simulation results under different grid numbers.

Grid Number	Node Number	Average Flow of Outlet (L/min)
454,430	792,420	97.552
567,169	1,045,980	99.975
735,362	1,312,560	100.067

It can be known from Table 4, when grid number is 454,000 and 567,000, the difference of the outlet average flow rate is 2.423 L/min, and difference rate is 2.5%. When grid number is 567,000 and 735,000, respectively, the difference of average flow rate is 0.092 L/min, and the difference rate is less than 0.1%. This deviation can be ignored. To speed up calculation speed, the grid model with grid number of 567,169 is selected for the numerical simulation.

3.4. Analysis of the Numerical Simulation Results

According to the relevant settings of aforementioned results, the simulation calculation of the flow channel model is performed. After the numerical simulation converged, we obtain the calculation results in the eighth cycle, such as the pressure cloud diagram on the symmetrical cross-section and the rotor section, the oil distribution area when absolute pressure is lower than 3000 Pa, the velocity vector diagram, the instantaneous and average flow rates curves, as shown below.

It can be known from Figure 12 that the oil films between the friction pairs completely separate the oil absorption cavity from the oil discharge cavity. The pressure distribution between the high and low pressure areas is uniformly transitioned. Thus, the applicability of the simulation model and the correctness of the simulation method are verified. In addition, when the rotation speed of the external gear is 2000 r/min, the corresponding minimum oil absorption pressure is 2259 Pa. This value is much less than atmospheric pressure, which indicates that the oil absorption process is very sufficient at this rotation speed. In addition, the corresponding maximum oil discharge pressure is 205,918 Pa, and this value is greater than the set pressure at the boundary, which will cause a certain degree of internal leakage.

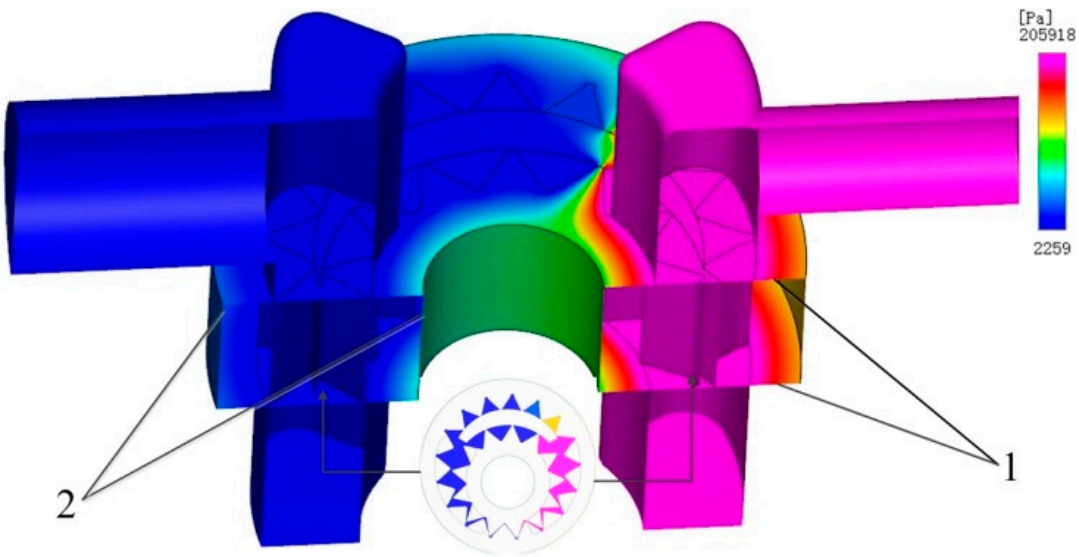

Figure 12. Pressure cloud diagram of the internal flow channel: 1–axial clearance; 2–radial clearance.

It can be known from Figure 13, when the absolute pressure is lower than 3000 Pa, the oil is all distributed in the oil absorption area, and concentrates in small area. This area is located after the front pair of gears withdraws the meshing, and far away from the oil absorption port. The oil is not sufficiently filled, so the established oil pressure is low in this area. In addition, due to the faster rotation speed of the external gear, there are also very small areas in the gap between the tooth tip circle and the crescent diaphragm.

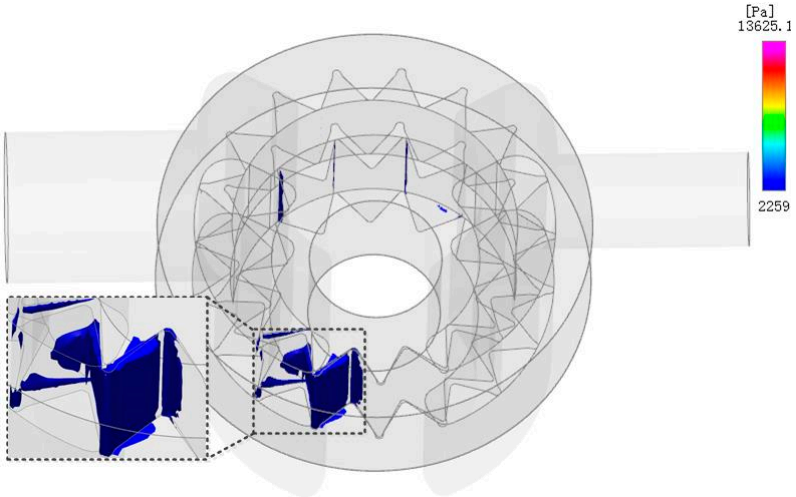

Figure 13. Oil distribution area when the absolute pressure is lower than 3000 Pa.

However, under the condition of oil working temperature is set at 30 °C and a certain amount of air is dissolved, the air separation pressure of the oil is about 1500 Pa. The saturated vapor pressure at this temperature is about 500 Pa [44]. Thus, the lowest pressure in the whole flow channel is higher than the air separation pressure of the oil. In addition, given that the highest oil pressure in the oil discharge area is only two atmospheric pressures. Therefore, the gas dissolved in the oil will not separate out, and the effective bulk modulus of elasticity will not change. Further, the oil compressibility has no effect on the flow pulsation and the average flow rate at outlet of the gear pump.

It can be known from Figure 14, under the meshing transmission of gear pair, the oil of the oil absorption cavity is continuously transported to the oil discharge cavity through interdental cavity. The oil velocity in the oil absorption area is relatively uniform, while the motion of fluid particles in the rotor area is complex and irregular. The oil velocity in the gap between the external gear, the internal gear ring and the crescent diaphragm, and between the gear surfaces is about 11 m/s, while the oil velocity in the rest is obviously lower. However, the high-speed oil has a great impact on the parts' surfaces, so it is necessary to implement the surfaces material modification of the gear surface and the surface of the crescent diaphragm. The oil distribution area is used to buffer the oil velocity in the oil absorption and oil discharge areas. The oil close to the oil absorption and oil discharge cavities has the gradually decreasing velocity, and the rest oil is in a static state. The oil in the oil discharge area first moves vertically upwards and then flows out horizontally along the outlet. Due to the large upward speed (approximately 7 m/s), it is difficult for the oil to make a smooth transition to the horizontal direction. Most oil passes along the upper wall of the outlet channel. Hence, increasing the wall thickness of the upper wall surface is necessary.

It can be known from Figure 15 that the instantaneous flow rate changes continuously and periodically, and there are 13 fluctuating pulsations. This is determined by the number of teeth on the driving gear (13). Secondly, unlike the theoretical instantaneous flow rate curve, the simulation instantaneous flow curve is not a smooth transition. The reason is that there is a certain gap between the surfaces of all friction pairs in the gear pump, and the gear side clearance changes constantly with the rotation of the gear pair. Therefore, the internal leakage from the clearances is inevitable. Furthermore, the non-uniformity of the internal leakage causes the gear pump to output a pulsating flow rate, and the pulsating flow rate changes periodically with the movement of the driving gear. Finally, according to the aforementioned analysis, under the working conditions applied in this study, the oil compressibility will not affect the flow pulsation at the outlet of the gear pump. In summary, the combined effect of the geometric flow pulsation and the uneven internal leakage leads to the instantaneous flow rate curve as shown in Figure 15.

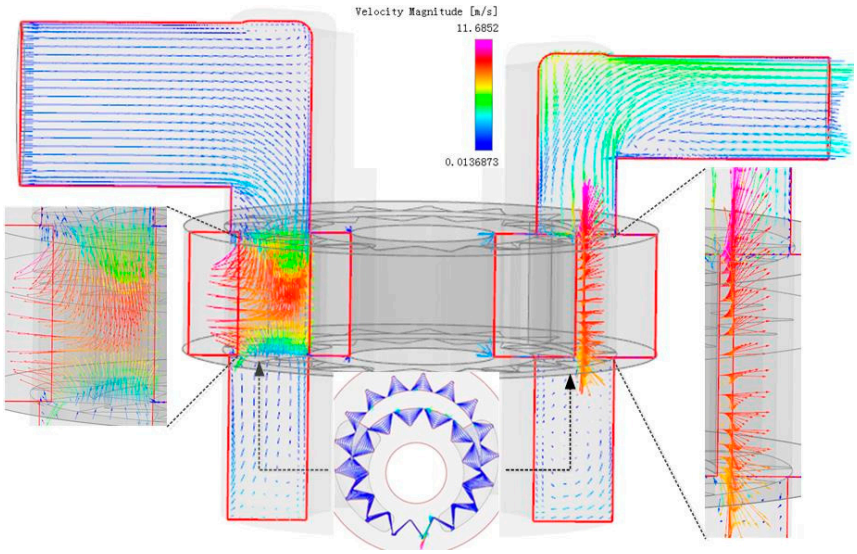

Figure 14. Velocity vector diagram of the cross-section.

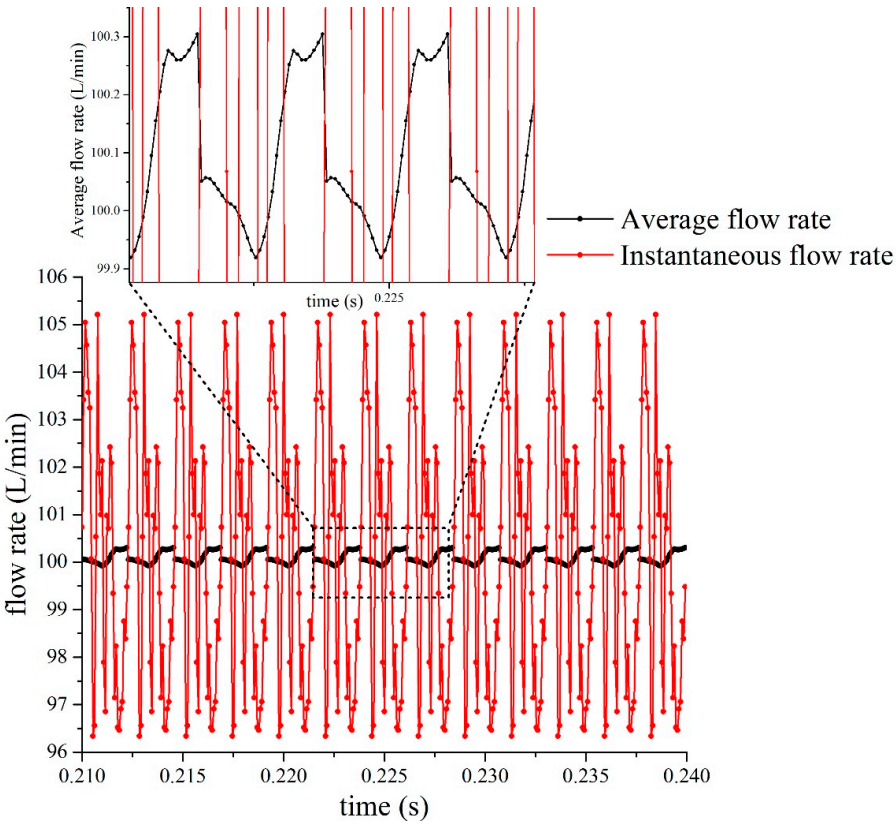

Figure 15. Instantaneous flow rate and average flow rate curves at the outlet of gear pump.

In addition, unlike the theoretical average flow rate curve, due to the pulsation of the instantaneous flow rate, the simulation average flow rate curve is also non-linear and changes periodically. However, the change of the average flow rate curve is very small (less than 0.4 L/min), which can be ignored compared with the instantaneous flow rate pulsation amplitude.

To further analyze the proportion of the flow pulsation caused by the geometric flow pulsation and the uneven internal leakage, the maximum, minimum, and average flow rates in Figure 15 are obtained, and the flow pulsation rate and the volume efficiency are calculated. In this way, the flow

characteristic data of the straight line conjugate internal meshing gear pump under no-load conditions are obtained, as shown in Table 5.

Table 5. Flow characteristic data under no-load conditions.

Maximum Flow Rate	Minimum Flow Rate	Average Flow Rate	Pulsation Rate	Volumetric Efficiency
(L/min)	(L/min)	(L/min)	(%)	(%)
105.21	96.34	100.12	8.86	99.52

It can be known from Table 5 that the total flow pulsation rate under no-load conditions is 8.86%. From the aforementioned results, the geometric flow pulsation rate is 1.76%, accounting for 19.9% of the total flow pulsation rate. In this way, the flow pulsation rate caused by the uneven internal leakage is 7.1%, accounting for 80.1%. Therefore, the uneven internal leakage is the main factor affecting the flow pulsation at the outlet of the gear pump.

In addition, the average flow rate calculated by the formula is 103.71 L/min. However, the average flow rate calculated by simulation is 100.12 L/min. The difference between the two is 3.59 L/min, and difference rate is 3.46%. The reason is that the internal leakage of oil is considered in the simulation calculation, and the leakage leads to the reduction of the simulation average flow rate.

4. Experimental Research on Flow Characteristics of a Straight Line Conjugate Internal Meshing Gear Pump

To further study the flow characteristics of the straight line conjugate internal meshing gear pump, a high-pressure (32 MPa) positive displacement test system is designed according to the test outline. According to the system schematic diagram, the required components are accurately selected and the physical objects are reasonably arranged. The operation of entire test bench is controlled by a computer, and all data is processed by professional software.

4.1. Overall Design of Test System

To realize the digital and automation requirements of data collection, the overall design scheme of the test system is arranged as shown in Figure 16.

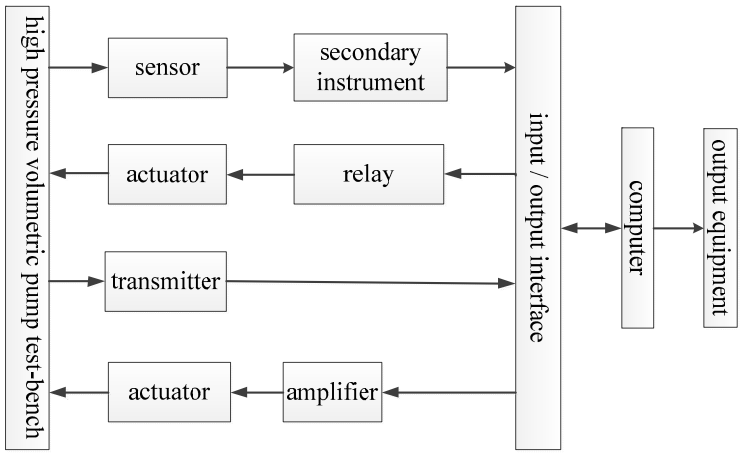

Figure 16. Overall design principle of test system.

It can be known from Figure 16 that the operation process of the test system is as follows: after the system is started, the signal is sent by the computer, and the test pump starts to run under the drive of variable frequency speed regulation three-phase asynchronous motor. The analog signal from the test pump is transmitted to the general input interface through each sensor and secondary instrument,

and directly or after conversion by the A/D converter is input to the computer, which is processed by the computer and stored in the database. The computer outputs the digital signal according to the program instructions, and then converts it to the analog signal after D/A converter. The analog signal is converted into a current signal by a proportional amplifier, which drives the relevant electronic control components of the test bench to operate. After the test is completed, the computer outputs the test results through the output device.

The hydraulic system design principle of the high-pressure positive displacement pump test bench in the test system is shown in Figure 17.

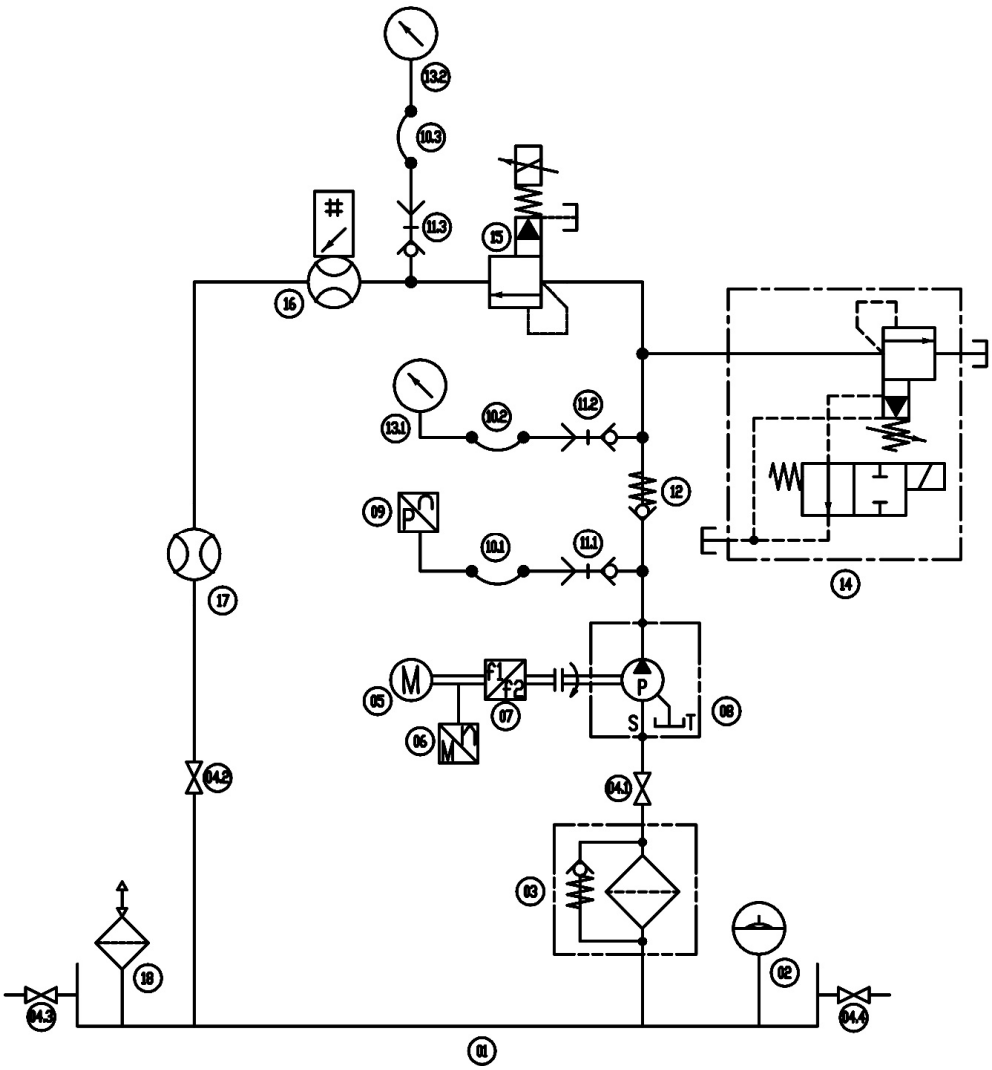

Figure 17. Design schematic diagram of hydraulic system: 01–tank; 02–level gauge; 03–suction filter; 04–shut–off valve; 05–variable frequency motor; 06–torque speed sensor; 07–frequency converter; 08–test pump; 09–pressure sensor; 10–pressure measuring hose; 11–pressure measuring connector; 12–check valve; 13–pressure gauge; 14–electromagnetic spill valve; 15–proportional relief valve; 16–digital flow meter; 17–flow meter; 18–air filter.

It can be known from Figure 17 that the hydraulic system is composed of power components, control components and hydraulic accessories, in which the power components are mainly composed of variable frequency motor (YVF2-55-2B35), test pump (QX41-050R), frequency converter (PR-F740-55K-CH), torque speed sensor (JC2C), torque meter (JW-3), and other components. The control components are mainly composed of check valve (TVP25-10), electromagnetic spill valve (DBW20B-1-50/31.5W220-50NZ5L), proportional relief valve (EBG-06-H), digital flowmeter

(FBLZJ-40-165J0), pressure sensor (FB3351GP0S22M3), and pressure gauge (YN-100-IV). The hydraulic accessories are mainly composed of level gauge (YWZ-350T), suction filter (TF-400 × 10L-Y), and shut-off valve (KH-G1/2″). The electromagnetic spill valve is used as a safety valve, and the system is in the unloading state before the electromagnet is energized. The proportional relief valve is installed in series on the main oil circuit, and the pressure of the test system is adjusted linearly according to the input current. The pressure sensor monitors total pressure at the outlet of the test pump in real-time. The two pressure gauges are arranged one behind the other of the proportional relief valve to accurately obtain the pressure loss of the system. Two digital flowmeters are installed in series in the main oil circuit, and the function of latter flowmeter is to check the measurement results of the previous flowmeter. The overall layout of the test system is shown in Figure 18.

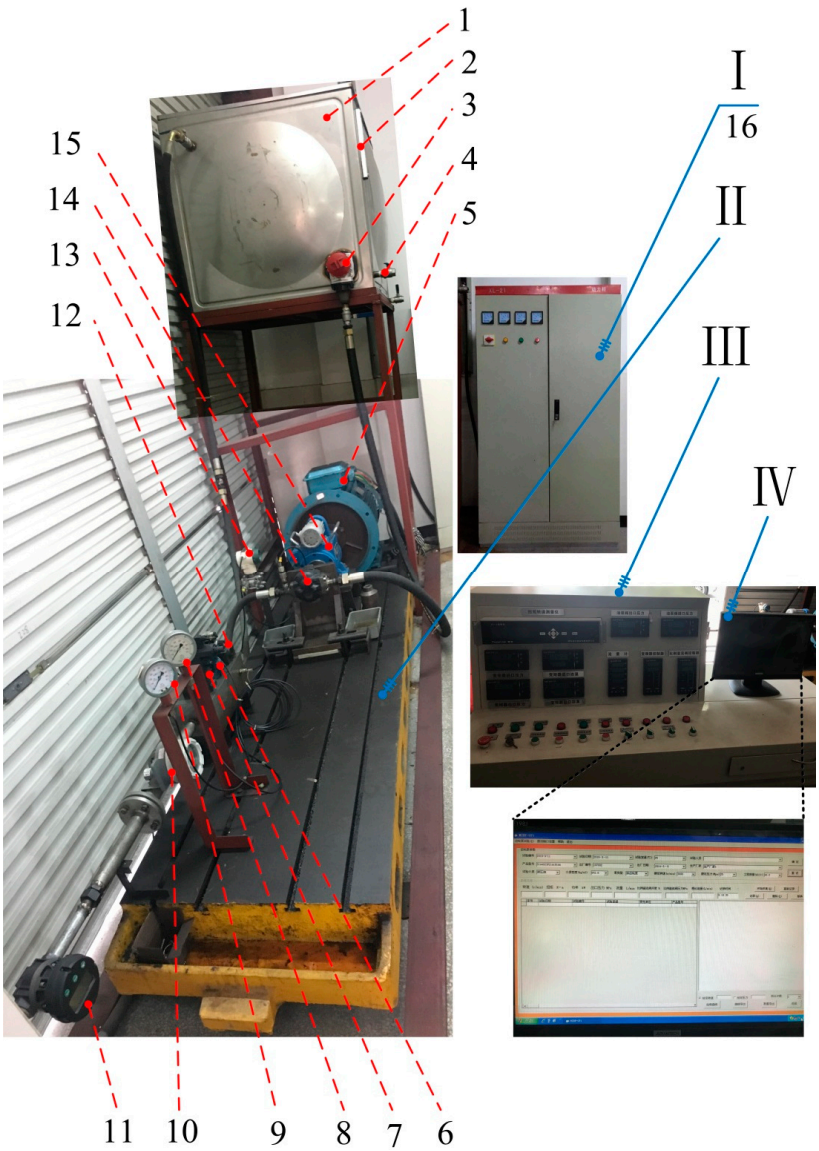

Figure 18. Overall layout of test system:I–test bench; II–power cabinet; III–control cabinet; IV–industrial computer; 1–tank; 2–level gauge; 3–suction filter; 4–shut-off valve; 5–variable frequency motor; 6–electromagnetic spill valve; 7–proportional relief valve; 8–pressure gauge 1; 9–pressure gauge 2; 10–digital flow meter; 11–flow meter; 12–check valve; 13–pressure sensor; 14–test pump; 15–torque speed sensor; 16–frequency converter.

It can be known from Figure 18 that the test system is composed of four parts: the test bench, the power cabinet, the control cabinet, and the industrial control computer. Among them, the frequency converter is installed in the power cabinet. After the test system is started normally, the current or voltage signal is keyed in the secondary instrument on the control cabinet, and then converted them into the corresponding driving signal through the proportional amplifier to control the action of the corresponding electrical components. The internally-developed data acquisition software is installed in the industrial computer to automatically save all data detected by the instruments.

4.2. Performance Evaluations and Result Analysis

With reference to the national test standard for the hydraulic gear pumps, the performance experiment content of the straight line conjugate internal meshing gear pump prototype is established, which mainly includes the running-in test. That is, the rotation speed of the frequency conversion motor is adjusted within the working speed range under the condition of no load. In this way, the assembled new pump can achieve the best working condition to avoid the problems such as over-tight fit or inflexible rotation. To be consistent with the conditions of simulation calculation, the test speed is also set to 2000 r/min, the working medium is also selected 46# hydraulic oil, and the performance evaluations are conducted at room temperature.

4.2.1. Analysis of the Outlet Average Flow Rate

In the course of the experiment, the prototype runs stably and no abnormal vibration and noise are found. Because the flow pulsation frequency ($z_1 n_1/60$) is very high, the current digital flowmeter cannot directly detect the instantaneous flow rate, and can only measure the average flow rate through the main oil circuit. Obtain the flowmeter's detection data within one minute and fit them into curve, as shown in Figure 19.

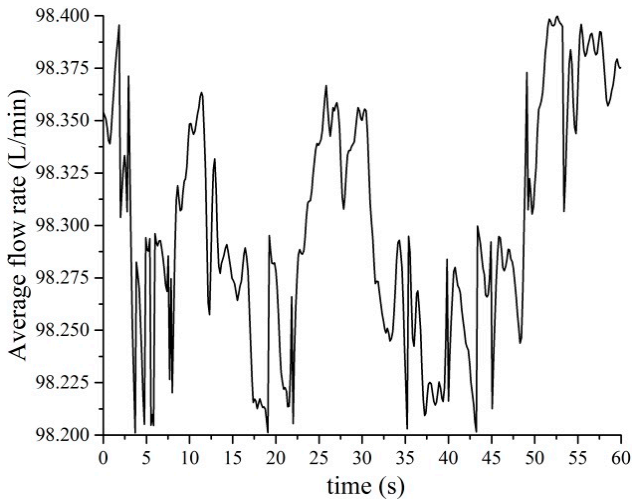

Figure 19. Average flow rate curve detected by the flowmeter.

It can be known from Figure 19, when the rotation speed of variable frequency motor is set to 2000 r/min, the average flow curve detected by the flowmeter is not a horizontal straight line, but fluctuates up and down with the passage of time, and the change amplitude is less than 0.2 L/min. The reason may be that the power supply of the frequency converter is unstable, the speed feedback is unstable, the program problem itself, and the harmonic content of external power supply is too high, etc. [45], which causes the speed of frequency conversion motor to fluctuate up and down within a certain range. Therefore, to obtain the average flow rate at a speed of 2000 r/min, average the flow rate within one minute, which is 98.30 L/min, and the corresponding volumetric efficiency is 97.71%. In this

way, the flow characteristics under no-load conditions obtained by theoretical analysis, numerical simulations, and experimental stufies can be listed, as shown in Table 6.

Table 6. Flow characteristics under no-load conditions.

Theoretical Calculation		Simulated Results		Experimental Results
Flow rate (L/min)	Flow pulsation rate (%)	Flow rate (L/min)	Flow pulsation rate (%)	Flow rate (L/min)
103.71	1.76	100.12	8.86	98.30

It can be known from Table 6, the experimental average flow rate decreases by 1.82 L/min when compared with the simulation average flow rate, which is due to factors such as the cumulative error of the measuring instruments and the large actual leakage. The decline rate is 1.8%, less than 2%, which can be ignored. The consistency between the simulation and experimental results verifies the applicability of the test system and the correctness of the test method.

4.2.2. Analysis of the Flow Rate-Speed Characteristic and Volume Efficiency–speed Characteristic

When the rotational speed of hydraulic pump is too low, the original small flow rate is almost all lost to the leakage. At this time, the hydraulic pump can hardly discharge the oil, the higher the pressure, the larger the leakage. Therefore, according to the minimum speed requirement of continuous output pressure in the gear pumps, and the table of the technical performance and the application range of hydraulic pumps [41,44], the speed range of the test pump is 750 r/min to 2600 r/min.

According to the running-in test method, the flow rate-speed and volume efficiency–speed characteristic curves of the gear pump at the main speeds of 750 r/min, 1000 r/min, 1500 r/min, 2000 r/min, and 2600 r/min are obtained, respectively, as shown in Figures 20 and 21.

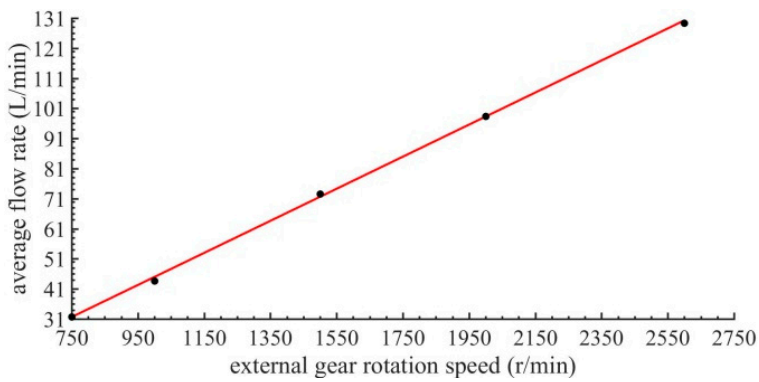

Figure 20. Flow rate-speed characteristic curve.

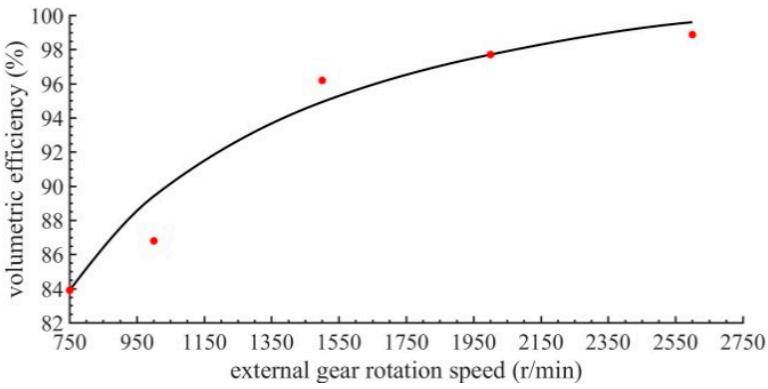

Figure 21. Volumetric efficiency–speed characteristic curve.

It can be known from Figure 20, under no-load conditions, the average flow rate at the outlet of the gear pump linearly increases with the increase in the rotation speed of the external gear, which is completely in line with the objective fact that the average flow rate of the fixed displacement pumps is proportional to the rotation speed. Since the internal leakage is different at different rotation speeds, further, the corresponding volumetric efficiency is also different. The specific volumetric efficiency–speed characteristic curve is shown Figure 21.

It can be known from Figure 21, under no-load conditions, with the increase in the rotation speed of the external gear, the volume efficiency increases as a logarithmic function with a base number greater than 1. When the rotation speed is greater than 1000 r/min, the corresponding volumetric efficiency is greater than 89%. When the rotation speed is greater than 1500 r/min, the corresponding volumetric efficiency is greater than 94%. When the rotational speed reaches the rated value of 2600 r/min, the corresponding volumetric efficiency is 98.87%, which is very close to 1. The reason is that the radial clearance leakage inside gear pump decreases slowly with the increase in the rotation speed, so the corresponding volumetric efficiency increases slowly.

Therefore, to increase the average flow rate at the outlet of the gear pump and improve the volumetric efficiency, the rotation speed of the external gear should be increased as much as possible within the allowable speed range.

5. Conclusions

In this paper, a general mathematical model of the theoretical instantaneous flow rate is established using the volume change method. By using the number-shape combination method, the theoretical instantaneous flow rate equations based on changes in the distance from the node to the meshing point and the rotation angle of the external gear, the initial and ending meshing angle equation sets, the theoretical coincidence degree equation, the theoretical oil trap time equation, the maximum and minimum instantaneous flow rate equations, the theoretical flow rate equation, and the geometric flow pulsation rate equation are analyzed and determined. Taking the straight line conjugate internal meshing gear pump as the research object, the theoretical flow rate curves that correspond to the theoretical and actual coincidence degrees are compared. Then, the specific values of the theoretical flow rate and the geometric flow pulsation rate are calculated and analyzed. The design variables affecting the theoretical flow rate and geometric flow pulsation rate and the corresponding value ranges are determined, and the change laws of the gear pair's geometric parameters on theoretical flow rate and geometric flow pulsation rate are studied. By using the dynamic grid technology in CFD and considering the clearance leakage of the axial and radial, the simulation model of the internal flow channel is developed. The numerical simulation results are analyzed and compared. The influence factors and the influence degree of the flow pulsation and the average flow rate at the outlet of the gear pump are investigated. The high-pressure positive displacement pump test system is also designed and built. The performance evaluations for the test pump are implemented, and the experimental results are analysed and compared with the simulation results. The specific conclusions are as follows:

1. The periodic change of the meshing point position is the root cause of the geometric flow pulsation. Gear pumps with different tooth profiles exhibit different flow pulsation characteristics. When the meshing point coincides with the node, the instantaneous flow rate reaches the maximum. When the rotation angle of the external gear is the same as the ending meshing angle, the instantaneous flow rate is at the minimum.
2. The ending meshing angle affects the instantaneous flow rate curves corresponding to the theoretical and actual coincidence degrees. On one hand, the theoretical instantaneous flow rate curve is smooth, and the geometric flow pulsation rate is low. On the other hand, the theoretical average flow rate curve is a straight line along the horizontal distribution. The theoretical coincidence degree is 1.1212, the theoretical flow rate is 103.71 L/min, and the geometric flow pulsation rate is 1.76%.

3. The tip circle radius of the external gear exerts the greatest influence on theoretical flow rate and geometric flow pulsation rate. As this radius increases, the theoretical flow rate sharply increases, and the geometric flow pulsation rate sharply decreases. The tip circle radius of the internal gear ring only influences the theoretical flow rate, which constantly decreases with the increase in this radius. The remaining variables exert no significant effect on theoretical flow rate and geometric flow pulsation rate. To increase the theoretical flow rate whilst decreasing the geometric flow pulsation rate, the tip circle radius of the external gear should be increased as much as possible within the allowable range of the design calculation.
4. The oil film between the surfaces of the friction pair separates the oil absorption cavity from the oil discharge cavity. The pressure distribution in the flow channel is evenly transitioned. The movement of fluid particles in the rotor area is in a complex and irregular state, and the oil velocity in the gap reaches the maximum value at 11 m/s. To prevent the erosion of high-speed oil, the surface material modification should be applied to the surfaces of the gear and the crescent diaphragm. The upper wall surface of the outlet channel is affected by the oil at a relatively high speed (approximately 7 m/s). Hence, increasing the wall thickness of the upper wall surface is necessary.
5. The factors that affect the flow pulsation include geometric flow pulsation, oil compressibility and uneven internal leakage. Under the working conditions applied in this study, the oil compressibility will not affect flow pulsation. The uneven internal leakage is the main influencing factor, accounting for 80.1% of the total flow pulsation rate. By contrast, the geometric flow pulsation only accounts for a small proportion (19.9%).
6. The factors that affect average flow rate are the oil compressibility and the internal leakage. Under the working conditions applied in this study, oil compressibility does not affect average flow rate. The internal leakage reduces the simulated average flow rate by 3.59 L/min compared with the theoretical flow rate. The simulated average flow rate curve demonstrates a non-linear periodic change with a small amplitude (less than 0.4 L/min).
7. The difference between the experimental and simulated average flow rates is 1.82 L/min. The difference rate is less than 2%. The consistency between the simulation and test results verifies the applicability of the test system and the correctness of the test method. Under no-load conditions, with the increase in the rotation speed of the external gear, the average flow rate linearly increases, and the volume efficiency increases as a logarithmic function with a base number greater than 1. To increase the average flow rate at the outlet of the gear pump and improve the volumetric efficiency, the rotation speed of the external gear should be increased as much as possible within the allowable speed range.

Future research on straight line conjugate internal meshing gear pumps will be conducted based on three aspects. Firstly, on the basis of the accurate equations are obtained in this study, taking the maximum theoretical flow rate and the minimum geometric flow pulsation rate as the objectives, the value range of the design variables is determined according to the constraint conditions. The design variables are sorted in the primary and secondary order based on orthogonal experiments. The multi-objective genetic algorithm is used to optimize the basic parameters of the gear pair. Secondly, given that the axial and radial clearances of the straight line conjugate internal meshing gear pump are fixed, the moving parts are sealed by a small fixed clearance. However, the internal leakage from the high-pressure cavity to the low-pressure cavity through the fixed gap is inevitable. When the clearance is small, the clearance leakage decreases, the velocity gradient of the liquid in the gap increases, and the viscous friction loss of the liquid increases. In contrast, when the clearance is large, the viscous friction loss of the liquid decreases, the leakage loss in the gap increases, and the volume efficiency decreases. The oil film thickness between the friction pair's surfaces becomes the main influencing factor of the dynamic characteristics and the volumetric efficiency of the gear pump. Lastly, the load capacity is one of important indicators in measuring the performance of gear pumps. The working pressure is an essential factor that affects the form and the content of air in hydraulic oil and is also the

main factor that changes the leakage flow rate. Moreover, this factor is a key source of pressure shock noises. The rotation speed change of the external gear under the loading conditions not only affects the average flow rate and the volume efficiency, but also influences the oil absorption characteristics and the oil properties. Consequently, the flow pulsation and the cavitation noise of gear pump are affected. In conclusion, the changes in the working parameters are essential influencing factors of the flow characteristics and working noises of gear pumps.

Author Contributions: Writing—original draft, writing—review and editing: H.C.; supervision, validation: G.Y.; formal analysis: G.W.; investigation, data curation: G.B.; conceptualization: W.L. All authors have read and agreed to the published version of the manuscript.

Funding: This research was funded by Open Foundation of the State Key Laboratory of Fluid Power and Mechatronic Systems, grant number GZKF-201823; Gansu Province Science and Technology Major Special Project-Research and Promotion of New Energy Comprehensive Utilization Technology, grant number 17ZD2GA010; Science and Technology Research Program of Chongqing Municipal Education Commission, grant number KJQN201801329; and The APC was funded by 17ZD2GA010.

Conflicts of Interest: The authors declare that they have no conflicts of interest.

Nomenclature

l	Vertical distance from external gear center to the tooth profile of the external gear	Z_2	Number of the internal gear ring
θ	Center angle corresponding to the gear thickness of the external gear reference circle	ω_1	Angular velocity of the external gear
β	Profile half angle of the external gear	ω_2	Angular velocity of the internal gear ring
r_1	Reference circle radius of the external gear	i_{12}	Gear pair transmission ratio
r_2	Reference circle radius of the internal gear ring	a	Center distance
B	Gear width	φ	Rotation angle of the external gear
r_{a1}	Tip circle radius of the external gear	Φ_0	Initial meshing angle
r_{f1}	Root circle radius of the external gear	Φ_1	Ending meshing angle
r_{a2}	Tip circle radius of the internal gear ring	φ_{lim}	Rotation angle of the external gear when the instantaneous flow rate reaches the limit
r_{f2}	Root circle radius of the internal gear ring	φ'	Angle between the line between the center of the external gear and the meshing point and the vertical axis
$\Delta\varphi_1$	Rotation angle of the external gear	n_1	Rotation speed of the external gear
$\Delta\varphi_2$	Rotation angle of the internal gear ring	ε_α	Coincidence degree
ΔV_1	Reduced volume of the oil discharge cavity	T_α	Theoretical oil trap time
ΔV_2	Enlarged volume of the oil discharge cavity	$\Delta\Sigma$	Oil discharge volume of each pair of gears
ΔV	Volume change of the oil discharge cavity	Σ	Theoretical displacement
q_{sh}	Theoretical instantaneous flow rate	q_t	Theoretical flow rate
ρ_1	Distance from the external gear center to the meshing point	q_{shmin}	Minimum instantaneous flow rate
ρ_2	Distance from the internal gear ring center to the meshing point	δ_q	Geometric flow pulsation rate
Z_1	Number of the external gear		

References

1. Castilla, R.; Gamez-Montero, P.J.; Del Campo, D.; Raush, G.; Garcia-Vilchez, M.; Codina, E. Three-dimensional numerical simulation of an external gear pump with decompression slot and meshing contact point. *Trans. ASME* **2015**, *137*, 539–550. [CrossRef]
2. Nishimoto, T. Noise, vibration and pulsation problems in oil hydraulic components and systems. *Thought-Evoking Approaches Eng. Probl. Toyama Jpn. Ohta-Kouyoudai* **2014**, *7*, 153–180.
3. Zhao, X.; Vacca, A. Numerical analysis of theoretical flow in external gear machines. *Mech. Mach. Theory* **2017**, *108*, 41–56. [CrossRef]

4. Zhao, X.; Vacca, A. Theoretical investigation into the ripple source of external gear pumps. *Energies* **2019**, *12*, 535. [CrossRef]
5. Chen, Z.; Lv, Z.; Xu, R.; Liao, J. Simulation and test of gear pump flow pulsation. *Mach. Syst.* **2018**, *11*, 265–272.
6. Truninger, P. Gear Pump. U.S. Patent 3,491,698, 27 January 1970.
7. Wang, W.; Yin, Y.-M.; He, S.-H.; Liu, G.-M. Study on flow characteristic of gear pumps by gear tooth shapes. *Appl. Sci. Eng.* **2017**, *20*, 367–372.
8. Huang, L.-Z. Tooth profile analysis of straight line-conjugate linetype internal meshing gear pump. *Mech. Transm.* **2004**, *28*, 16–22.
9. Dong, Y.-C.; Cui, J.-K.; Li, K.; Wei, Z. Study on sliding ratio of the straight conjugate internal gear pair. *Mach. Des. Manuf.* **2006**, *7*, 9–12.
10. Cong, X.-Q.; Liu, M.-X.; Wu, J. Design method of straight conjugate Internal gear pump. *Drain. Irrig. Mach.* **2008**, *26*, 33–36.
11. Zhang, Y.-S.; Hu, X.-H.; Liu, Y.-B.; Chen, L. The study of straight conjugate internal meshing gear pump. *Mach. Des. Manuf.* **2010**, *6*, 138–140.
12. Liu, L.-C. Gear's Research and Analysis of the Linear Conjugated Internal Gear Pump. Master's Thesis, Tianjin University of Technology, Tianjin, China, 2014.
13. Xu, X.-Z.; Zhang, K.; Tan, H.-M. Research on mesh characteristics of straight conjugated internal gear pump. *Mach. Tool Hydraul.* **2011**, *39*, 48–51.
14. Yang, G.-Y.; Bai, G.-X. The tooth profile equation of straight conjugate internal gear pump based on pressure angle function. *Hydraul. Pneum.* **2012**, *7*, 39–42.
15. Wei, W.-F.; Zhang, G.-P.; Du, Z.-Y.; Kang, N. Design method of internal rotary gear pump by parameterized line conjugated tooth profile. *J. Mech. Eng.* **2014**, *50*, 49–55. [CrossRef]
16. Gu, K.-L.; Wang, Z.-H.; Li, G.; Liu, X.-R. Optimization of geometric parameters of the straight conjugate internal gear pump based on GA. *Electron. Sci. Technol.* **2017**, *30*, 39–44.
17. Hu, H.-L.; Cui, J.-K.; Xu, J.-B. Optimal design of tooth profile parameter of straight-conjugate internal gear pair. *Mech. Transm.* **2015**, *39*, 77–80.
18. Li, X.; Cui, J.-K. Analysis of the interference of straight conjugate internal gear pair based on matlab. *Mech. Transm.* **2014**, *38*, 128–131.
19. Xu, X.-X.; Song, T.-L. Optimal design of basic parameters of straight line conjugate gear pump. *Mech. Transm.* **2007**, *31*, 69–72.
20. Rundo, M. Models for flow rate simulation in gear pumps: A review. *Energies* **2017**, *10*, 1261. [CrossRef]
21. Zhao, X.; Vacca, A. Analysis of continuous-contact helical gear pumps through numerical modeling and experimental validation. *Mech. Syst. Signal Process.* **2018**, *109*, 352–378. [CrossRef]
22. Pellegri, M.; Vacca, A. Numerical simulation of gerotor pumps considering rotor micro-motions. *Meccanica* **2016**, *52*, 1851–1870. [CrossRef]
23. Li, S.-D.; Cui, J.-K. The finite element analysis of pump body line. *Manuf. Autom.* **2011**, *33*, 33–37.
24. Wang, Z.-W.; Zhang, Z.-S.; Liang, W.-G.; Zhang, F. Analysis on meshing efficiency of straight conjugate internal gear pair. *Torpedo Technol.* **2013**, *21*, 369–374.
25. Xu, X.-Z.; Song, T.-L. Study on sliding coefficients of straight line conjugate tooth profile gear pairs. *J. Huaiyin Teach. Coll.* **2007**, *3*, 225–228.
26. Yuan, D.-Q.; Kang, S.-B.; Cong, X.-Q.; Liu, M. Finite element analysis on gear tangency stress of straight line conjugate internal gear pump. *Drain. Irrig. Mach.* **2009**, *27*, 111–114.
27. Gao, M.-L.; Cui, J.-K.; Huang, D.-P.; Liu, S.; Zhang, L. The calculation analysis of contact ratio for straight conjugate internal gear transmission. *Fluid Mach.* **2017**, *45*, 28–32.
28. Duan, G.; Cui, J.-K.; Gao, M.-L. Contact ratio of an internal meshing gear pair with a straight line tooth profile out gear. *J. Univ. Shanghai Sci. Technol.* **2018**, *40*, 335–341.
29. Rundo, M. Theoretical flow rate in crescent pumps. *Simul. Model. Pract. Theory* **2017**, *71*, 1–14. [CrossRef]
30. Rundo, M.; Corvaglia, A. Lumped parameters model of a crescent pump. *Energies* **2016**, *9*, 876. [CrossRef]
31. Rydlewicz, W.; Rydlewicz, W.; Pałczyński, T. Experimental investigation of the influence of an orifice plate on the pressure pulsation amplitude in the pulsating flow in a straight pipe. *Mech. Syst. Signal Process.* **2019**, *117*, 634–652. [CrossRef]

32. Liu, D.-W.; Ba, Y.-B.; Ren, T.-Z. Flow fluctuation abatement of high-order elliptical gear pump by external noncircular gear drive. *Mech. Mach. Theory* **2019**, *134*, 338–348. [CrossRef]
33. Wang, Z.-L.; Zhang, Z.-S.; Zhang, F.-F.; Liu, J. Analysis of the effect of parameter on trapping oil of straight conjugate internal gear pump. *Mech. Transm.* **2014**, *38*, 91–93.
34. Xu, X.-Z.; Song, T.-L. Analysis of flow characteristics of gear pump with straight line profile. *Coal Min. Mach.* **2008**, *29*, 47–50.
35. Wang, Z.-W.; Cui, J.-K.; Zhang, L.-H. Instantaneous flow analysis of straight line conjugate internal meshing gear pump. *Fluid Transm. Control* **2013**, *4*, 23–27.
36. Zhang, H.; Wang, Z.-H. Analysis of the flow pulsation of straight conjugated internal gear pump. *Mech. Transm.* **2015**, *39*, 98–102.
37. Kilani, M.I. Computer aided design tools in the development of surface micromachined mechanisms. *Jordan J. Mech. Ind. Eng.* **2011**, *5*, 167–176.
38. Zhang, Y. The Research of New Processing Method in Large Module Internal Engage Gear Based on Conjugate Principle. Master's Thesis, Dalian University of Technology, Dalian, China, 2007.
39. Wei, B.; Xiong, H.-G. *Gear Mechanism and Its Design. Mechanical Principle*, 1st ed.; Huazhong University of Science & Technology Press: Wuhan, China, 2007; Volume 7, pp. 137–180.
40. Chen, Y.-Q.; Xue, D.-Y. *Basic Programming of MATLAB Language. System Simulation Technology and Application Based on MATLAB/Simulink*, 2nd ed.; Tsinghua University Press: Beijing, China, 2002; Volume 2, pp. 17–93.
41. Buch Hydraulics. *Technical Data & Performance Graphs. High Pressure Internal Gear Pumps*; Buch Hydraulics Co. Ltd.: Bern, Switzerland, 2014; Volume 2 & 3, pp. 5–10.
42. Xu, Y.-M. *Oil Film Design in Gears and Vane Pumps (Motors). Oil Film Theory and Friction Pair Design of Hydraulic Pumps and Motors*, 1st ed.; Machinery Industry Press: Beijing, China, 1987; Volume 13, pp. 354–381.
43. Jiang, Y.; Furmanczyk, M.; Lowry, S.; Zhang, D.; Perng, C.-Y. *A Three-Dimensional Design Tool for Crescent Oil Pumps*; SAE World Congress & Exhibition: Detroit, MI, USA, 2008; pp. 4–14.
44. Wang, Y.-Q.; Gao, D.-R. *Hydraulic Medium. Technical Manual for Hydraulic Engineers*, 1st ed.; Chemical Industry Press: Beijing, China, 2009; Volume 2, pp. 66–71.
45. Rao, S.-H. *Asynchronous Motor. Electrical and Electronic Technology Foundation*, 1st ed.; Beijing Institute of Technology Press: Beijing, China, 2008; Volume 6, pp. 103–119.

© 2020 by the authors. Licensee MDPI, Basel, Switzerland. This article is an open access article distributed under the terms and conditions of the Creative Commons Attribution (CC BY) license (http://creativecommons.org/licenses/by/4.0/).